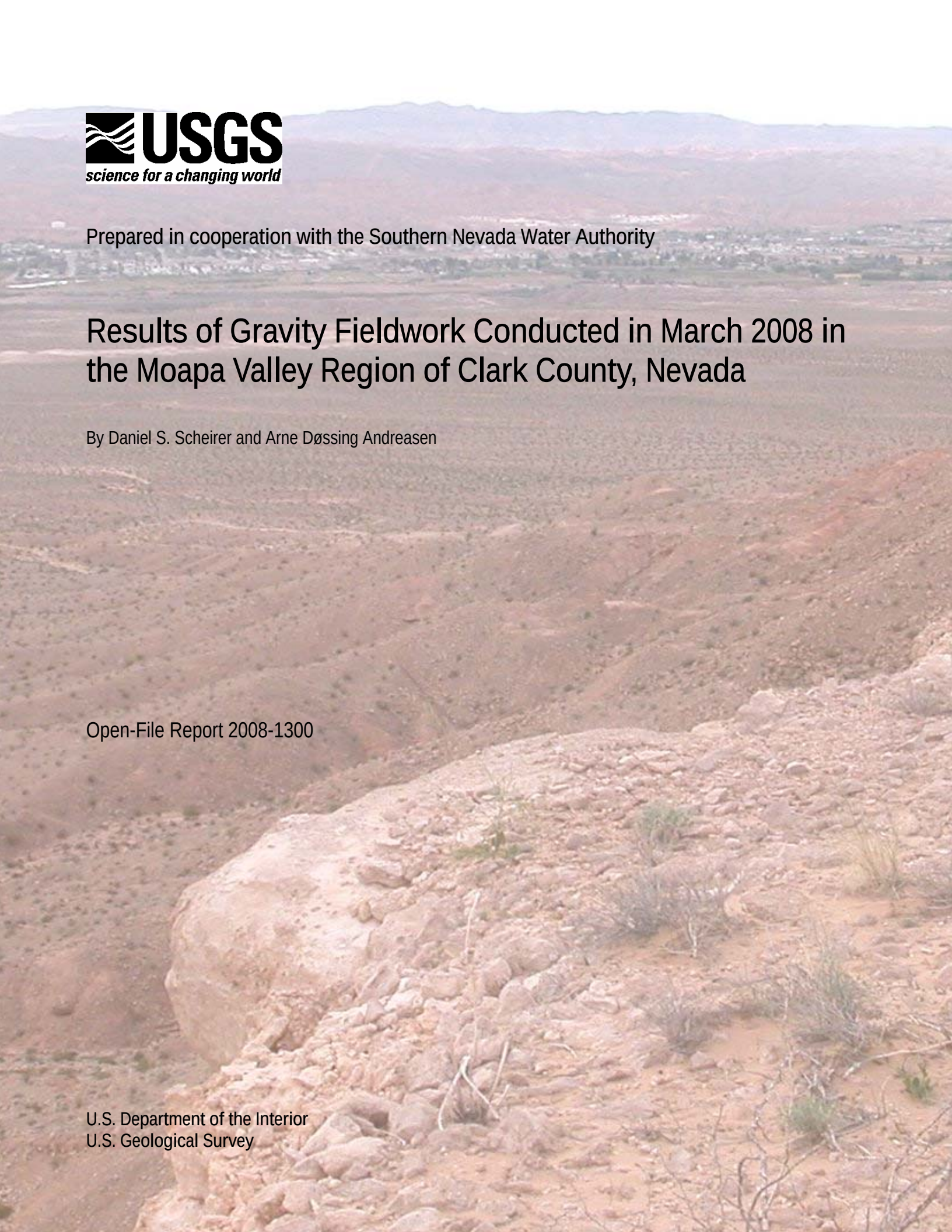

USGS
science for a changing world

Prepared in cooperation with the Southern Nevada Water Authority

Results of Gravity Fieldwork Conducted in March 2008 in the Moapa Valley Region of Clark County, Nevada

By Daniel S. Scheirer and Arne Døssing Andreasen

Open-File Report 2008-1300

U.S. Department of the Interior
U.S. Geological Survey

U.S. Department of the Interior
DIRK KEMPTHORNE, Secretary

U.S. Geological Survey
Mark D. Myers, Director

U.S. Geological Survey, Reston, Virginia 2008

For product and ordering information:
World Wide Web: http://www.usgs.gov/pubprod
Telephone: 1-888-ASK-USGS

For more information on the USGS—the Federal source for science about the Earth,
its natural and living resources, natural hazards, and the environment:
World Wide Web: http://www.usgs.gov
Telephone: 1-888-ASK-USGS

Suggested citation:
Scheirer, D.S., and Andreasen, A.D., 2008, Results of gravity fieldwork conducted in March 2008 in the Moapa Valley region of Clark County, Nevada: U.S. Geological Survey Open-File Report 2008-1300, 35 p. [http://pubs.usgs.gov/of/2008/1300/].

Contents

Figures

Tables

Conversion Factors

Inch/Pound to SI

Multiply	By	To obtain
	Length	
inch (in.)	2.54	centimeter (cm)
inch (in.)	25.4	millimeter (mm)
foot (ft)	0.3048	meter (m)
mile (mi)	1.609	kilometer (km)
mile, nautical (nmi)	1.852	kilometer (km)
yard (yd)	0.9144	meter (m)

SI to Inch/Pound

Multiply	By	To obtain
	Length	
centimeter (cm)	0.3937	inch (in.)
millimeter (mm)	0.03937	inch (in.)
meter (m)	3.281	foot (ft)
kilometer (km)	0.6214	mile (mi)
kilometer (km)	0.5400	mile, nautical (nmi)
meter (m)	1.094	yard (yd)

Results of Gravity Fieldwork Conducted in March 2008 in the Moapa Valley Region of Clark County, Nevada

By Daniel S. Scheirer[1] and Arne Døssing Andreasen[2]

[1]U.S. Geological Survey, Menlo Park, California, USA

[2]Geologisk Institut, Copenhagen University, Copenhagen, Denmark

Abstract

In March 2008, we collected gravity data along 12 traverses across newly-mapped faults in the Moapa Valley region of Clark County, Nevada. In areas crossed by these faults, the traverses provide better definition of the gravity field and, thus, the density structure, than prior gravity observations. Access problems prohibited complete gravity coverage along all of the planned gravity traverses, and we added and adjusted the locations of traverses to maximize our data collection. Most of the traverses exhibit isostatic gravity anomalies that have gradients characteristic of exposed or buried faults, including several of the newly-mapped faults.

Introduction

The flow and storage of ground water in southern Nevada is governed by the geological units and structures that integrate the long and complex history of deposition, deformation, and erosion of this region. Recently, new high-resolution mapping of faults in and around Moapa Valley (fig. 1; G.L. Dixon and P.D. Rowley, oral commun., 2008) suggests that a nexus of structures may influence ground water in the vicinity of the lowermost Pahranagat Wash and Muddy River. Although some of these faults are parallel to the regional strike of geological units and the basin-bounding normal faults (fig. 2), the longer newly-mapped faults cross the regional geological strike, and they may be important for interbasin ground water flow (fig. 1). These newly mapped faults are denoted as “terminus” for the long faults marked in green in figure 1 and other figures, and “GE7C” for shorter faults marked in yellow.

A synthesis of geologic mapping in this area was compiled at a regional scale (1:250,000; Page and others, 2005; fig. 2). Interpretive geologic cross-sections were generated by Page and others (2006), focusing on the lithologic and structural features that allow or impede ground water flow in southern Nevada. Cross-sections D-D’, E-E’, and I-I’ by Page and others (2006) are closest to the March 2008 study area. Regional geophysical studies, using primarily gravity but also seismic and magnetic analyses, are presented by Langenheim and others (1999), Phelps and others (2000), Langenheim and others (2000), Langenheim and others (2001a,b), and Scheirer and others (2006).

Gravity Fieldwork

In late March 2008, the U.S. Geological Survey (USGS) collected gravity observations at 266 sites to supplement the prior compilation of stations in this area (fig. 3; Ponce, 1997; Langenheim and others, 1999; Scheirer and others, 2006). We used two gravimeters: a Scintrex CG-5 Autograv meter and the LaCoste-Romberg meter G8-N. During each field day, we read the meters at gravity base station OVER (Best Western North Shore Inn, Overton, Nev.; established in November 1998; IGSN71 gravity value of 979,656.90 mGal; Langenheim and others, 1999) at the beginning and end of the day. In addition, most days we read gravity base station GLEN (Glendale Motel, Glendale, Nev.; established in May 2000; IGSN71 gravity value of 979,682.63; Phelps and others, 2000) before and after collecting field stations. The gravity stations collected in this area by the USGS in the past decade have been referenced to either OVER or GLEN. The gravity stations referenced to GLEN are shown as pink symbols in figure 3. Figures 4 and 5 show expanded views of the March 2008 and prior gravity stations in the northwestern and southeastern portions, respectively, of the study area.

Gravity stations were collected along 12 transects crossing the newly-mapped faults in the study region (fig. 1). Because the southern half of Line 4 crossed the grounds of a power plant, we also collected stations along a roadway to the east of the plant, and labeled this alternative Line 4se. Gravity stations were initially collected at 0.2 mile (~320 m) spacing, and later fill-in stations were added to achieve 0.1 mile (~160 m) spacing along portions of many of the lines. Most stations were collected along roadways and tracks, although about 5 percent of the stations were collected by foot, mainly at the ends of lines where driving was impossible. We collected stations only on public lands. Gravity stations were collected by using two field-teams and were numbered using two prefixes: 08lr, for LaCoste-Romberg G8-N observations and 08cg, for Scintrex CG-5 observations.

In addition to the gravity observations, we collected high-resolution GPS locations using hand-held Trimble GPS units that allow post-processed differential corrections to achieve sub-meter location precisions. One unit was a single-GPS-frequency GeoXT, with vertical precisions of about 1 m; the other unit was a dual-GPS-frequency GeoXH, with vertical precisions generally less than 0.5 m. In the process of calculating gravity anomalies, the uncertainty in station elevation is most often the greatest source of uncertainty in the resulting gravity anomalies. Sub-meter elevation precision allows confidence in elevation corrections to ~0.2 mGal.

At each gravity station, we estimated the magnitude of the terrain correction to the simple Bouguer term, within a radius of 175 feet (53.3 m; Hammer C). These field terrain corrections are added to those calculated for more distant areas by using digital elevation models (DEMs). For the most part, we tried to collect gravity stations >175 feet from significant topography, and we assigned these stations a nominal field terrain correction of 0.01 mGal. For sites where we could not avoid being closer than 175 feet, we estimated the terrain corrections from a graph of displaced-slope terrain corrections (Plouff, 2000). At five stations where the close topography could not be estimated with the displaced-slope graph, we sketched the adjacent topography and calculated the resulting field terrain correction digitally (Plouff, 2000). At one gravity station, 08lr016, an extreme field terrain correction >2 mGal was estimated in a steep-sided canyon near the northern limit of access along Line 1 in Wildcat Wash.

Table 2 in the appendix contains the principal facts of the gravity stations collected in March 2008. A digital file of these data is provided as a supplement to this report.

Gravity Processing

Gravity readings were corrected for instrument calibration factors, fluctuations related to tidal accelerations, and instrument drift constrained at the beginning and end of each field day. Observed gravity values were referenced to the OVER base station, using the International Gravity Standardization Net of 1971 (IGSN 71) gravity datum (Morelli, 1974). We compared the GPS-measured station elevations to interpolated elevations from USGS 10-m DEMs. In all but one case, the station elevations differed by less than 12 m from the DEM value. The single exception was station 08lr053, which had an elevation ~22 m lower than the DEM value; this exception arises because this station was collected near the base of the Overton Beach boat ramp into Lake Mead, which extends well below the normal Lake Mead pool elevation of 366 m that is assigned to the DEM. Station 08lr053 will be omitted from complete Bouguer and isostatic gravity anomaly analysis because the DEM-based terrain correction algorithm does not account for changing lake levels.

We calculated a series of predictable gravity effects at each station accounting for the global gravity field, the reduction in gravity with increasing elevation (free-air correction), the effect of mass between the station and the geoid (simple Bouguer correction), the effect of the earth's curvature (curvature correction), the effect of topographic variation near the station (terrain correction), and the effect of compensating mass near the base of the crust (isostatic correction). The final gravity anomaly after application of these effects is termed the isostatic gravity anomaly, and it is useful for interpretation because it primarily reflects the density variations in the upper- and mid-crust (Simpson and others, 1986). For all stations, digital terrain corrections beyond 53.3 m were calculated from DEMs in two stages, from 53.3 m to 2 km and from 2 km to 167 km, using the algorithm of Plouff (1977). Other parameters that were used in the calculation of predictable gravity effects are typical for gravity studies in the Great Basin; these include an upper crustal density of 2.67 g/cm^3, a mantle-crust density contrast of 0.4 g/cm^3, and a nominal crustal thickness at sea level of 25 km.

We projected the March 2008 gravity stations onto best-fit lines to generate profiles along the gravity traverses; these profiles are the primary results described below. In addition, we extended the traverse lines by 2 km on each end and projected prior gravity stations that fell within 1 km of the extended traverse as part of the profile analysis. Finally, we extracted elevations along the traverse from a DEM and calculated the intersections of each profile with the newly mapped faults and with roadways.

Below, we provide brief descriptions of issues of access and manmade features along each line, information that might be helpful for future geophysical work in this area. We also documented many of the lines with digital photographs; while not incorporated into this report, they may prove helpful for planning future work.

Rock Samples

At 4 gravity stations situated on outcrop, we collected hand samples and measures their density (Johnson and Olhoeft, 1984) and magnetic susceptibility properties in the lab (table 1). These measurements supplement those of prior studies (for example, Langenheim and others, 1999; Scheirer and others, 2006), and they may be used to guide gravity and magnetic modeling. While physical properties of hand-samples may not individually represent well the bulk properties of in situ volumes of rock, especially those at depth, the measurements can aid in establishing realistic density variations among the lithologic units for gravity analysis.

The densities and magnetic susceptibilities of three of the four samples are within the normal range for these lithologies, although the calcrete sample (QTc, 08lr089) is more magnetic than most

carbonate samples. The one sample of a Quaternary spring-apron deposit (Qsa, 08cg019) has a markedly low density and high lab-derived porosity (18%).

Results

Gravity Setting

The most recent isostatic gravity compilation containing the study area was presented by Scheirer and others (2006) and is illustrated in figure 6. This map shows the correlation of ranges with positive gravity anomalies and of basins with negative gravity anomalies (compare fig. 6 with fig. 1). The Mormon and Virgin Mountains have the most positive gravity anomalies in the area due to the presence of dense Proterozoic basement in the shallow subsurface. The Virgin River Depression coincides with some of the most negative gravity anomalies in the entire Basin and Range province (Langenheim and others, 2001a). Gravity lines 1, 2, and 3 lie on the gravity high that connects the southernmost Meadow Valley Mountains with the Arrow Canyon Range (fig. 6). Line 11 crosses the gradient between that gravity high and a low associated with Meadow Valley Wash. Line 4 lies in the transition between basins associated with California Wash and lowermost Meadow Valley Wash. Line 5 lies along a gravity high joining the Mormon Mountains with the Northern Muddy Mountains. Line 6 lies at the edge of the basin associated with the Overton Arm of Lake Mead, and Line 7 lies at a basement high separating that basin with the "Mormon subbasin" of the Virgin River Depression. Lines 8, 9, 10, and 12 lie within the Mormon subbasin, and the northeast end of line 10 lies near the inferred maximum depth of the subbasin beneath Mormon Mesa (fig. 6).

At the regional gravity scale of figure 6, it is difficult to see any correlations between the gravity field based on the prior gravity observations and the newly-mapped fault structures that cross the main basin-range physiography. As can be seen in figure 7 for each gravity line, the definition of the gravity field has been improved greatly by the March 2008 campaign relative to what was available from prior data.

We expect to see faults, exposed at the surface or buried, with gravity observations if they juxtapose units having different densities. This is often the case with dip-slip faults where unconsolidated and semiconsolidated sediments are juxtaposed against higher-density bedrock. This density contrast may sometimes be the case for strike-slip faults that cut dipping beds or that have large-offset. The absence of a gravity anomaly associated with a mapped or inferred strike-slip fault does not necessarily argue against the existence of this fault; rather, the density contrast across a fault may not be great enough to produce an observable gravity anomaly at the land surface. For a fault that juxtaposes units having significantly different densities, the location of the shallow limit of its density contrast coincides with a maximum lateral gradient in the gravity anomaly. In addition, if the gravity signature of a fault is superimposed on a regional gradient, the fault signature may be associated with deviations from a smooth gravity gradient. In figure 7, these gradient locations are highlighted on each gravity traverse with labels of more-confident (F) and less-confident (F?) fault picks.

Line 1

Line 1 extends from just south of Pahranagat Wash northward along Wildcat Wash until that wash closes into a slot canyon where transporting a gravimeter became impossible. This is a location where pictographs are visible in the sculpted carbonate walls (probable Ordovician Pogonip Group limestone). The isostatic gravity anomaly has a symmetric U-shape (fig. 7) with a minimum slightly more than 1-km south of Nevada 168. There is no apparent gravity gradient associated with the

"terminus" cross-fault that coincides with Pahranagat Wash. A one-station negative gravity deviation near a profile distance of 3.4 km may be associated with a buried fault, but additional data would need to be acquired to confirm this suggestion.

Logistic notes: The stations within and south of Pahranagat Wash were collected while walking because this is a wilderness area. A power transmission line is situated ~100 m south of Nevada 168, which approximately parallels the roadway; otherwise, manmade features were absent.

Line 2

Line 2 extends from just south of Pahranagat Wash northward along Deadman Wash. The isostatic gravity anomaly increases irregularly going to the north (fig. 8). A ~2.5 mGal gravity step is centered a few hundred meters south of the "terminus" cross-fault that coincides with Pahranagat Wash; this is the best example of a gravity signature that coincides with one of the newly-mapped faults. Another ~1.5 mGal step near the northern limit of the line is likely related to a fault, and a deviation in the gravity gradient at a profile distance of ~2 km might also be fault-related.

Logistic notes: The stations within and south of Pahranagat Wash were collected while walking because this is a wilderness area. Some stations north of Nevada 168 were also collected by walking, where no drivable tracks were present. A power transmission line is situated ~200 m south of Nevada 168, which approximately parallels the roadway; otherwise, manmade features were absent.

Line 3

Line 3 has an isostatic gravity anomaly with an irregular U-shape (fig. 9), reflecting the proximity to Paleozoic outcrop seen in figure 2. A negative gravity deviation (~0.5 mGal, profile distance of -0.1 km) from a linear isostatic gravity gradient is associated with the cross-fault that extends along Muddy Wash, although the significance of this deviation is unknown. Another deviation near ~1.1 km may be fault-related. The high-gradient at the northern end of the line is likely to be related to a fault, although additional gravity data along the track heading north would be needed to verify this interpretation.

Logistic notes: A power transmission line is situated ~500 m north of Nevada 168, which approximately parallels the roadway. The unpaved roadway north of NV168 has a decreasing amount of manmade features driving to the north; the roadway south of NV168 is paved and is associated with fences, parallel power-lines, and bridges.

Line 4

Line 4 has an isostatic gravity anomaly with a symmetric, inverted U-shape (fig. 10) that likely reflects the basement high separating California Wash from lowermost Meadow Valley Wash (fig. 6). No deviations of the isostatic gravity anomaly are associated with the cross-fault that extends along Muddy River.

Logistic notes: The gravity stations along Line 4 occur along a curved roadway, and the southern stations are adjacent to the Reid Gardner Power Plant. Power-transmission lines extend outwards in all directions from this power plant. To the north of NV168, the roadway parallels a railroad track and power lines, and it passes a manufacturing plant.

Line 4se

Line 4se has an isostatic gravity anomaly that decreases steadily to the north (fig. 11), reflecting its location on the transition from the basement high connecting the northern Muddy Mountains with the

Mormon Mountains to the gravity low of lowermost Meadow Valley Wash (fig. 6). A small deviation of the isostatic gravity anomaly is associated with the cross-fault (marked in green in fig. 11) that extends along Muddy River; additional data between the existing stations would improve the definition of the gravity gradient associated with this fault.

Logistic notes: Line 4se coincides with Line 4 in its northern half, but it deviates to the southeast in its southern half to avoid the Reid Gardner Power Plant. The gravity stations along Line 4se occur along a curved roadway. Power-transmission lines extend outwards in all directions from the power plant. To the north of NV168, the roadway parallels a railroad track and power lines, and it passes a manufacturing plant.

Line 5

Line 5 has an isostatic gravity anomaly that increases steadily to the north (fig. 12). No deviations of the isostatic gravity anomaly are associated with the cross-fault that extends along Muddy River. A one-station positive gravity anomaly at 2 km may be a minor expression of a fault, but additional observations are needed to verify this. The fault indicated in figure 7.05 at ~3.4 km crosses the gravity profile at an oblique angle.

Logistic notes: Line 5 does not coincide with many drivable tracks between Interstate 15 and the Muddy River. Much of the data collection in this section of the line was done while walking, and on one occasion the truck became stuck in loose sand and needed to be dug out. Line 5 crosses a power-transmission line midway between Muddy River and I-15, and it crosses a railway near the Muddy River.

Line 6

Line 6 does not cross the "terminus" fault that extends along the northwestern tip of the Overton Arm of Lake Mead. Line 6 has an isostatic gravity anomaly that decreases steadily to the east in a sigmoidal fashion (fig. 13), reflecting entry into the basin coincident with the Overton Arm.

Logistic notes: Line 6 extends along the paved Overton Beach Road of Lake Mead National Recreation Area, which has occasional gates and fences along its length. The eastern stations occur near a visitor center/boat ramp/parking lot complex. Because of the low-lake level (~22 m below the normal pool elevation), the easternmost station, 08lr053, extended several hundred meters from the shoreline marked on USGS topographic maps.

Line 7

The western portion of Line 7 extends toward but does not cross the "terminus" fault which lies along the northwestern tip of the Overton Arm of Lake Mead. The western portion of Line 7 has an isostatic gravity anomaly (fig. 14) that mimics the sigmoidal anomaly of Line 6. The eastern portion of Line 7 has an anomaly reflecting a portion of the northeastern edge of the basin coincident with the Overton Arm. Because closely-spaced stations in Line 7 do not cross the "terminus" fault, it is difficult to know if any gravity signature is associated with that fault.

Logistic notes: Line 7 extends along the unpaved road leading to the old St. Thomas site in Lake Mead National Recreation Area, which crosses a power line. After a gap of ~5.5 km, the stations extend to the northeast along a road that leads to the "Narrows", approaching from the Virgin Mountains side. While topographic maps indicate Lake Mead separating these groups of stations, the lowered lake level has yielded a grassy plain across this gap. Gravity stations could be collected on this plain, including at the abandoned and formerly-submerged St. Thomas site, to cross the "terminus" fault (green in fig. 14).

Line 8

Access to Line 8 was limited by private property to the southeast and by thick brush and no roadways northeast of Muddy River. Some gravity stations were collected in the process of determining these limitations, but the line will not be interpreted in this study (fig. 15). Two stations on Mormon Mesa were collected collinear with the portion of Line 8 along Kaolin Wash.

Line 9

Southeast of Muddy River in Magnesite Wash, the isostatic gravity anomaly has a hump (fig. 16). Unfortunately, access immediately northeast of the "terminus" fault was impossible, so the gravity behavior at that fault is unknown. The gaps in gravity coverage northeast of the Muddy River prevent definitive interpretation of gravity along this half of the line. Two stations on Mormon Mesa were collected collinear with the portion of Line 9 in Moapa Valley.

Logistic notes: Line 9 extends along an unpaved road up Magnesite Wash to the southwest. Some power-lines and homes are present along the lower reaches of the wash. An abandoned mine site lies at the southwestern end of the line. A railroad, power lines, and other man-made structures occur near NV169. Gravity stations between 2-3 km were collected near the sewage-treatment plant, which had buildings, power lines, and fences.

Line 10

The isostatic gravity anomaly of Line 10 is marked by a near-linear decrease towards the northeast (fig. 17). No noticeable gravity behavior is associated with crossing the "terminus" fault near Muddy River, but a ~1 mGal step near -1.2 km may arise from a buried fault.

Logistic notes: Line 10 extends along an unpaved road up Overton Wash to the southwest. Some power-lines and homes are present along the lower reaches of the wash, and on two occasions, audible shooting prevented collection at a couple of the southwestern-most planned sites. The central portion of Line 10 was collected within the town of Overton, with residential and commercial buildings and infrastructure.

Line 11

The isostatic gravity anomaly of Line 11 is marked by a near-linear decrease towards the east (fig. 18). No noticeable gravity behavior is associated with crossing the "terminus" faults.

Logistic notes: Line 11 extends along several paved roads near Muddy and Warm Springs. Some power lines and ranches are present along the line.

Line 12

The isostatic gravity anomaly of Line 12 is irregular (fig. 19). A small (<0.5 mGal) gravity anomaly may be associated with crossing the "terminus" fault near Muddy River, but this correlation is not definitive. Two other gradient changes have been labeled as possible buried fault locations.

Logistic notes: Most of Line 12 extends along a paved road to the sewage treatment plant. Power-lines, homes, and fences are present along most of the line.

Unresolved Issue

The published observed gravity value at base station GLEN (Phelps and others, 2000) appears to be 0.29 mGal too high, based on results from the March 2008 fieldwork. This result was first noticed

when we collected multiple OVER→GLEN ties with both meters on the initial field days. To establish this offset more rigorously and to determine whether the gravity values at GLEN, OVER, or both were in error, we conducted a double-loop tie of these stations to base station MESCN in Mesquite, Nev. on March 28, 2008 with two LaCoste-Romberg gravity meters: G8-N and G425. Based on real-time calculations, it appeared that the OVER value was consistent with MESCN and that the GLEN value was in error. The estimated error value of 0.29 mGal was determined after processing the data incorporating the instrument calibration factors. We confirmed the approximate magnitude and sense of the GLEN error by re-occupying two gravity stations collected in 2002 that were referenced to GLEN.

For the gravity stations collected in March 2008, we omitted the GLEN ties from the calculations and used only the OVER base ties. To blend the March 2008 data as seamlessly as possible with prior USGS-collected gravity data, we may need to shift the gravity values of the prior stations referenced to GLEN by the 0.29 mGal value. This shifting has not been done, but would be advisable before revised grids and depth-to-basement solutions are created.

Guidance for Future Work

A natural extension of the work would be to quantitatively model the gravity profiles by using 2-dimensional and 2+1/2-dinensional forward modeling techniques. Such modeling should incorporate mapped geology and lithologic density values consistent with hand-sample measurements (for example, table 1 and similar observations).

To expand this analysis in an areal manner would require creating new isostatic gravity grids, which would be a first step to quantitative depth-to-basement analysis. To improve such areal analysis, the adjustment of prior gravity station values derived from the GLEN gravity base, noted above, would need to be accomplished.

To improve both two-dimensional and areal gravity analysis, acquiring gravity data at locations along the traverses with high gravity gradients would help characterize buried faults. In a few cases, extending the gravity traverses would aid in characterizing faults that are inferred to exist near the edges of the existing traverses. In addition, collecting gravity observations along traverses that fill gaps between the existing traverses (especially between Lines 5 and 10) would help in following the continuity of faults inferred from the existing gravity coverage.

Acknowledgments

We thank the Southern Nevada Water Authority for project funding. We thank the University of Copenhagen for funding Andreasen's visit at the USGS. We are very grateful to Keith Pari and Todd Gurnee for their assistance in the field and to Gary Dixon for proposing and aiding this work. We thank Ed Mankinen and Darcy McPhee for technical reviews.

Table 1. Physical property measurements of rock samples collected in March 2008 in southern Nevada.

[Latitude and longitude use NAD27 datum]

Sample identification	Rock type, map unit on Page and others (2005)	Latitude north	Longitude west	Grain density, in g/cm^3	Saturated bulk density, in g/cm^3	Dry bulk density, in g/cm^3	Porosity, In percent	Susceptibility In 10^{-3} SI
08cg074	Sandstone, Tru	36°37.37’	114°32.88’	2.63	2.53	2.48	6.0	0.10
08lr016	Limestone, Oep	36°48.40’	114°51.08’	2.69	2.66	2.65	1.3	0.04
08lr019	Limestone, Qsa	36°47.80’	114°51.29’	2.38	2.17	2.01	18.0	0.02
08lr089	Limestone, QTc	36°32.56’	114°23.45’	2.60	2.60	2.60	0.3	0.25

References Cited

Johnson, G.R., and Olhoeft, G.R., 1984, Density of rocks and minerals, *in* Carmichael, R.S., ed., CRC Handbook of Physical Properties of Rocks, v. 3: Boca Raton, Fla., CRC Press, Inc., p. 1-38.

Langenheim, V.E., Davidson, J.G., Anderson, M.L., and Blank, H.R., Jr., 1999, Principal facts for gravity stations and physical property measurements in the Lake Mead 30' by 60' quadrangle, Nevada and Arizona: U.S. Geological Survey Open-File Report 99-435, 26 p.

Langenheim, V.E., Glen, J.M., Jachens, R.C., Dixon, G.L., Katzer, T.C., and Morin, R.L., 2000, Geophysical constraints on the Virgin River depression, Nevada, Utah, and Arizona: U.S. Geological Survey Open-File Report 00-407, 26 p.

Langenheim, V.E., Bohannon, R.G., Glen, J.M., Jachens, R.C., Grow, J.A., Miller, J.J., Dixon, G.L., and Katzer, T.C., 2001a, Basin configuration of the Virgin River depression, Nevada, Utah, and Arizona—A geophysical view of deformation along the Colorado Plateau-Basin and Range transition, in Erskine, M.C., Faults, J.E., Bartley, J.M., and Rowley, P.D., eds., The geologic transition, High Plateaus to Great Basin-A symposium and field guide (The Mackin Volume): Utah Geological Association and Pacific Section of the American Association of Petroleum Geologists: Utah Geological Association Publication 30, p. 205-226.

Langenheim, V.E., Miller, J.J., Page, W.R., and Grow, J.A., 2001b, Thickness and geometry of Cenozoic deposits in California Wash area, Nevada, based on gravity and seismic reflection data: U.S. Geological Survey Open-File Report 01-393, 24 p.

Morelli, C., 1974, The International Gravity Standardization Net 1971: International Association of Geodesy Special Publication no. 4, 194 p.

Page, W.R., Dixon, G.L., Rowley, P.D, and Brickey, D.W., 2005, Geologic map of parts of the Colorado, White River, and Death Valley ground water flow systems, Nevada, Utah, and Arizona: Nevada Bureau of Mines and Geology Map 150, 1:250,000-scale.

Page, W.R., Scheirer, D.S., Langenheim, V.E., 2006, Geologic cross sections of parts of the Colorado, White River, and Death Valley regional ground-water flow systems, Nevada, Utah, and Arizona: U.S. Geological Survey Open-File Report 2006-1040, 23 p.

Phelps, G.A., Jewel, E.B., Langenheim, V.E., and Jachens, R.C., 2000, Principal facts for gravity stations in the vicinity of Coyote Spring Valley, Nevada, with initial gravity modeling results: U.S. Geological Survey Open-File Report 00-420, 18 p.

Plouff, D., 1977, Preliminary documentation for a FORTRAN program to compute gravity terrain corrections based on topography digitized on a geographic grid: U.S. Geological Survey Open-File Report 77-535, 45 p.

Plouff, D., 2000, Field estimates of gravity terrain corrections and Y2K-compatible method to convert from gravity readings with multiple base stations to tide- and long-term drift-corrected observations: U.S. Geological Survey Open-File Report 2000-140, 37 p.

Ponce, D.A., 1997, Gravity data of Nevada: U.S. Geological Survey Digital Data Series DDS-42, 27 p, CD-ROM.

Scheirer, D.S., Page, W.R., and Miller, J.J., 2006, Geophysical studies based on gravity and seismic data of Tule Desert, Meadow Valley Wash, and California Wash basins, southern Nevada: U.S. Geological Survey Open-File Report 2006-1396.

Simpson, R.W., Jachens, R.C., Blakely, R.J., and Saltus, R.W., 1986, A new isostatic residual gravity map of the conterminous United States with a discussion on the significance of isostatic residual anomalies: Journal of Geophysical Research, v. 91, p. 8348-8372.

Appendix

Table 2. Principal facts of gravity stations collected in March 2008 in the Moapa Valley region of southern Nevada.

[Datums: latitude and longitude, NAD27; elevations, NGVD29. FAA, free-air gravity anomaly; ITC, inner terrain correction calculated out to 2 km; TTC, total terrain correction; CBA, complete Bouguer gravity anomaly; ISO, isostatic gravity anomaly]

Station	Latitude north (degrees)	Longitude west (degrees)	Elevation (m)	Observed gravity (mGal)	FAA (mGal)	ITC (mGal)	TTC (mGal)	CBA (mGal)	ISO (mGal)
08cg001	36.5853	-114.4048	572.1	979614.22	-78.06	0.63	0.65	-142.14	-33.23
08cg002	36.5805	-114.4123	477.8	979634.87	-86.08	0.23	0.23	-139.93	-31.27
08cg003	36.5785	-114.4158	466.0	979637.39	-87.03	0.14	0.16	-139.61	-31.08
08cg004	36.5767	-114.4190	459.6	979638.71	-87.54	0.09	0.12	-139.44	-31.01
08cg005	36.5752	-114.4215	454.6	979639.75	-87.91	0.07	0.11	-139.26	-30.92
08cg006	36.5728	-114.4238	447.0	979641.30	-88.50	0.06	0.11	-138.99	-30.78
08cg007	36.5707	-114.4263	439.6	979643.00	-88.91	0.05	0.11	-138.55	-30.44
08cg008	36.5683	-114.4288	431.2	979644.84	-89.44	0.08	0.16	-138.09	-30.07
08cg009	36.5665	-114.4308	423.0	979646.85	-89.80	0.06	0.16	-137.53	-29.60
08cg010	36.5650	-114.4327	415.1	979648.52	-90.44	0.06	0.18	-137.25	-29.38
08cg011	36.5630	-114.4355	411.2	979649.79	-90.21	0.04	0.17	-136.59	-28.82
08cg012	36.5620	-114.4368	408.8	979650.33	-90.33	0.04	0.17	-136.43	-28.71
08cg013	36.5613	-114.4385	407.0	979650.81	-90.35	0.04	0.17	-136.24	-28.56
08cg014	36.5600	-114.4407	404.0	979651.57	-90.39	0.04	0.18	-135.95	-28.33
08cg015	36.5573	-114.4428	389.5	979654.81	-91.38	0.06	0.27	-135.21	-27.67
08cg016	36.5552	-114.4423	388.0	979655.46	-91.01	0.22	0.44	-134.49	-27.01
08cg017	36.5532	-114.4425	387.8	979655.47	-90.91	0.02	0.24	-134.57	-27.14
08cg018	36.5523	-114.4425	384.7	979655.59	-91.66	0.02	0.26	-134.95	-27.54
08cg019	36.5508	-114.4425	386.5	979655.78	-90.78	0.02	0.25	-134.29	-26.92
08cg020	36.5497	-114.4425	385.9	979655.88	-90.78	0.02	0.25	-134.21	-26.86
08cg021	36.5485	-114.4425	385.8	979656.18	-90.39	0.02	0.25	-133.82	-26.51
08cg022	36.5463	-114.4458	386.0	979656.61	-89.73	0.02	0.26	-133.17	-25.96
08cg023	36.5453	-114.4472	386.3	979656.93	-89.21	0.02	0.26	-132.69	-25.54
08cg024	36.5445	-114.4483	387.6	979656.96	-88.73	0.03	0.26	-132.35	-25.24
08cg025	36.5437	-114.4492	388.5	979656.86	-88.46	0.03	0.26	-132.19	-25.11
08cg026	36.5425	-114.4505	391.9	979656.79	-87.39	0.05	0.27	-131.49	-24.45
08cg027	36.5408	-114.4510	390.1	979656.49	-88.11	0.05	0.28	-131.99	-25.01
08cg028	36.5403	-114.4523	393.2	979656.43	-87.16	0.07	0.29	-131.39	-24.42
08cg029	36.5388	-114.4542	394.5	979656.22	-86.85	0.11	0.33	-131.18	-24.28
08cg030	36.5383	-114.4560	397.2	979655.72	-86.46	0.18	0.39	-131.03	-24.16
08cg031	36.5372	-114.4583	400.8	979655.29	-85.70	0.52	0.73	-130.33	-23.49
08cg032	36.5372	-114.4610	404.9	979654.45	-85.25	0.55	0.76	-130.33	-23.50
08cg033	36.5347	-114.4625	406.6	979653.59	-85.37	0.19	0.40	-131.00	-24.25
08cg034	36.5320	-114.4638	413.7	979652.01	-84.54	0.19	0.38	-130.99	-24.30
08cg035	36.5293	-114.4647	420.2	979650.65	-83.67	0.21	0.37	-130.86	-24.26
08cg036	36.5267	-114.4658	425.1	979649.56	-83.00	0.31	0.46	-130.66	-24.15
08cg038	36.7527	-114.8218	614.9	979648.80	-44.77	0.51	1.37	-112.96	8.36
08cg039	36.7557	-114.8213	620.6	979647.61	-44.47	0.60	1.40	-113.28	8.16
08cg040	36.7585	-114.8217	626.5	979646.73	-43.77	0.65	1.41	-113.24	8.32
08cg041	36.7610	-114.8197	632.2	979645.78	-43.19	0.50	1.21	-113.50	8.06
08cg042	36.7638	-114.8182	639.5	979644.48	-42.47	0.19	0.85	-113.97	7.64
08cg043	36.7667	-114.8167	647.9	979642.97	-41.63	0.12	0.73	-114.19	7.48

08cg044	36.7695	-114.8158	652.5	979641.99	-41.43	0.20	0.80	-114.44	7.30
08cg045	36.7718	-114.8137	660.9	979641.07	-39.98	0.08	0.65	-114.09	7.67
08cg046	36.7747	-114.8122	668.8	979640.10	-38.76	0.07	0.61	-113.80	8.04
08cg047	36.7775	-114.8108	676.0	979638.85	-38.02	0.08	0.60	-113.88	8.02
08cg048	36.7802	-114.8097	681.1	979638.16	-37.37	0.15	0.67	-113.74	8.23
08cg049	36.7827	-114.8093	688.5	979637.82	-35.64	0.11	0.62	-112.90	9.16
08cg050	36.7850	-114.8098	693.5	979637.19	-34.95	0.15	0.65	-112.73	9.47
08cg051	36.7873	-114.8098	699.9	979635.85	-34.49	0.12	0.62	-113.04	9.27
08cg052	36.7887	-114.8095	702.7	979635.31	-34.31	0.12	0.62	-113.17	9.19
08cg053	36.7675	-114.7212	615.5	979657.38	-37.30	0.17	0.55	-106.38	12.33
08cg054	36.7645	-114.7200	610.3	979659.08	-36.94	0.21	0.57	-105.41	13.12
08cg055	36.7623	-114.7182	603.9	979659.54	-38.25	0.17	0.52	-106.06	12.32
08cg056	36.7593	-114.7177	596.0	979660.20	-39.78	0.13	0.48	-106.73	11.51
08cg057	36.7563	-114.7182	590.5	979660.56	-40.85	0.09	0.44	-107.23	10.90
08cg058	36.7533	-114.7187	585.8	979661.55	-41.07	0.07	0.41	-106.93	11.07
08cg059	36.7505	-114.7180	580.4	979662.40	-41.62	0.05	0.39	-106.90	10.94
08cg060	36.7473	-114.7185	573.7	979663.93	-41.90	0.06	0.41	-106.40	11.29
08cg061	36.7445	-114.7192	569.0	979664.30	-42.72	0.06	0.42	-106.68	10.91
08cg062	36.7420	-114.7210	561.9	979665.66	-43.33	0.09	0.49	-106.42	11.12
08cg063	36.7408	-114.7220	559.3	979666.01	-43.68	0.11	0.53	-106.44	11.08
08cg064	36.7387	-114.7250	557.2	979666.11	-44.04	0.14	0.59	-106.50	10.99
08cg065	36.7363	-114.7273	552.5	979667.11	-44.29	0.17	0.66	-106.15	11.31
08cg066	36.7343	-114.7290	551.0	979667.69	-43.99	0.07	0.59	-105.76	11.65
08cg067	36.7303	-114.7288	550.5	979668.57	-42.94	0.08	0.60	-104.63	12.60
08cg068	36.7270	-114.7290	550.8	979668.68	-42.45	0.13	0.65	-104.12	12.95
08cg069	36.7218	-114.7293	581.4	979662.34	-38.88	0.40	0.78	-103.89	12.94
08cg070	36.7193	-114.7287	585.3	979662.00	-37.80	0.26	0.63	-103.40	13.30
08cg071	36.6732	-114.5345	492.9	979675.23	-49.11	0.20	0.28	-104.60	6.78
08cg072	36.6180	-114.5498	505.3	979665.74	-49.99	1.01	1.16	-106.02	3.28
08cg073	36.6205	-114.5500	498.8	979667.30	-50.65	0.89	1.05	-106.05	3.32
08cg074	36.6228	-114.5480	490.0	979669.15	-51.70	1.06	1.23	-105.94	3.51
08cg075	36.6253	-114.5457	483.0	979671.10	-52.12	0.95	1.12	-105.68	3.86
08cg076	36.6278	-114.5442	476.5	979672.32	-53.14	1.22	1.39	-105.68	3.94
08cg077	36.6307	-114.5442	472.7	979673.81	-53.07	1.35	1.53	-105.05	4.66
08cg078	36.6337	-114.5443	464.4	979675.98	-53.73	0.85	1.05	-105.23	4.60
08cg079	36.6367	-114.5438	458.3	979677.89	-53.94	0.64	0.86	-104.95	4.98
08cg080	36.6395	-114.5438	455.7	979678.53	-54.35	0.42	0.65	-105.28	4.76
08cg081	36.6455	-114.5412	453.9	979679.37	-54.60	0.29	0.49	-105.48	4.79
08cg082	36.6482	-114.5403	456.3	979679.38	-54.09	0.32	0.50	-105.23	5.14
08cg083	36.6507	-114.5398	457.4	979679.63	-53.69	0.35	0.52	-104.95	5.53
08cg084	36.6538	-114.5393	462.9	979679.03	-52.87	0.37	0.51	-104.76	5.83
08cg085	36.6555	-114.5395	464.7	979678.84	-52.65	0.28	0.41	-104.84	5.82
08cg086	36.6588	-114.5397	468.0	979678.88	-51.89	0.30	0.42	-104.44	6.34
08cg087	36.6617	-114.5383	473.2	979678.59	-50.83	0.28	0.38	-104.00	6.92
08cg088	36.6640	-114.5377	474.6	979678.09	-51.09	0.19	0.30	-104.51	6.51
08cg089	36.6665	-114.5355	480.8	979677.28	-50.20	0.22	0.31	-104.31	6.80
08cg090	36.5078	-114.4372	392.9	979657.18	-83.68	0.08	0.24	-127.92	-21.60
08cg091	36.5080	-114.4338	386.8	979658.08	-84.69	0.07	0.25	-128.23	-21.86
08cg092	36.5082	-114.4303	381.9	979658.93	-85.36	0.07	0.26	-128.34	-21.91
08cg093	36.5100	-114.4282	381.4	979658.88	-85.73	0.04	0.23	-128.68	-22.17
08cg094	36.5155	-114.4233	377.5	979659.17	-87.12	0.02	0.22	-129.63	-22.95
08cg095	36.7555	-114.8250	623.6	979647.82	-43.33	0.26	1.09	-112.78	8.77

08cg096	36.7543	-114.8257	619.5	979648.07	-44.23	0.31	1.18	-113.14	8.40
08cg097	36.7538	-114.8258	619.8	979647.94	-44.21	0.37	1.24	-113.09	8.44
08cg098	36.7528	-114.8272	637.4	979643.87	-42.77	0.40	1.18	-113.69	7.84
08cg099	36.7500	-114.8270	690.1	979631.89	-38.25	0.35	0.92	-115.39	6.00
08cg100	36.7488	-114.8282	709.1	979627.70	-36.47	0.60	1.15	-115.52	5.87
08cg101	36.7517	-114.8283	655.5	979639.13	-41.82	0.45	1.16	-114.81	6.71
08cg102	36.7188	-114.7272	580.8	979662.47	-38.69	0.25	0.63	-103.78	12.84
08cg103	36.7200	-114.7290	582.9	979662.34	-38.28	0.27	0.65	-103.58	13.15
08cg104	36.7248	-114.7290	551.9	979667.94	-42.66	0.20	0.72	-104.39	12.57
08cg105	36.7285	-114.7288	549.8	979668.70	-42.86	0.11	0.63	-104.44	12.70
08cg106	36.7317	-114.7288	551.8	979668.00	-43.22	0.07	0.58	-105.07	12.20
08cg107	36.7332	-114.7288	552.1	979667.97	-43.29	0.06	0.57	-105.19	12.15
08cg108	36.7355	-114.7282	554.1	979667.29	-43.56	0.05	0.54	-105.72	11.72
08cg109	36.7377	-114.7265	556.5	979666.86	-43.43	0.08	0.55	-105.85	11.64
08cg110	36.7393	-114.7233	569.9	979663.99	-42.32	0.04	0.42	-106.39	11.09
08cg111	36.6620	-114.6227	492.4	979667.82	-55.70	0.03	0.09	-111.34	0.46
08cg112	36.6588	-114.6203	492.6	979669.02	-54.16	0.04	0.10	-109.81	1.86
08cg113	36.6560	-114.6178	486.5	979671.57	-53.24	0.03	0.11	-108.19	3.32
08cg114	36.6523	-114.6123	474.0	979676.23	-52.13	0.04	0.18	-105.60	5.68
08cg115	36.6525	-114.6062	473.3	979677.47	-51.12	0.05	0.19	-104.49	6.68
08cg116	36.6470	-114.6008	505.8	979671.05	-47.01	0.07	0.12	-104.14	6.75
08cg117	36.6420	-114.6010	514.7	979670.03	-44.86	0.07	0.11	-103.00	7.66
08cg118	36.6383	-114.6005	521.0	979669.45	-43.19	0.05	0.09	-102.05	8.45
08cg119	36.5355	-114.4422	386.1	979657.18	-88.18	0.04	0.25	-131.64	-24.68
08cg120	36.5355	-114.4403	384.1	979657.20	-88.79	0.03	0.25	-132.02	-25.03
08cg121	36.5355	-114.4385	383.2	979657.22	-89.05	0.03	0.25	-132.18	-25.18
08cg122	36.5353	-114.4362	385.2	979657.16	-88.46	0.04	0.24	-131.83	-24.79
08cg123	36.5353	-114.4345	381.1	979657.24	-89.64	0.02	0.24	-132.55	-25.48
08cg124	36.5353	-114.4332	380.5	979657.26	-89.82	0.02	0.24	-132.66	-25.56
08cg125	36.5355	-114.4315	381.2	979657.18	-89.70	0.02	0.24	-132.62	-25.51
08cg126	36.5355	-114.4297	380.8	979657.18	-89.80	0.02	0.24	-132.68	-25.54
08cg127	36.5353	-114.4278	379.0	979657.33	-90.19	0.02	0.25	-132.86	-25.70
08cg128	36.5353	-114.4262	378.4	979657.44	-90.27	0.03	0.26	-132.85	-25.66
08cg129	36.5353	-114.4245	378.9	979657.63	-89.95	0.03	0.26	-132.58	-25.37
08cg130	36.5353	-114.4227	378.8	979657.82	-89.77	0.05	0.29	-132.37	-25.13
08cg131	36.5352	-114.4200	382.4	979657.42	-89.06	0.07	0.30	-132.06	-24.79
08cg132	36.5355	-114.4177	393.1	979655.34	-87.86	0.05	0.24	-132.13	-24.81
08cg133	36.5355	-114.4152	391.9	979655.86	-87.71	0.06	0.26	-131.81	-24.44
08cg134	36.5355	-114.4128	398.0	979654.68	-87.02	0.07	0.25	-131.82	-24.44
08cg135	36.5355	-114.4105	403.5	979653.65	-86.34	0.09	0.26	-131.76	-24.34
08cg136	36.5353	-114.4087	413.0	979651.78	-85.26	0.10	0.23	-131.78	-24.33
08cg137	36.5358	-114.4068	419.3	979650.67	-84.48	0.12	0.24	-131.71	-24.23
08cg138	36.5358	-114.4047	421.1	979650.10	-84.48	0.14	0.26	-131.90	-24.37
08cg139	36.5365	-114.4025	431.2	979648.12	-83.41	0.18	0.27	-131.96	-24.39
08cg140	36.5323	-114.4100	399.2	979654.20	-86.84	0.08	0.26	-131.77	-24.43
08cg141	36.5225	-114.4298	380.7	979658.20	-87.72	0.02	0.22	-130.59	-23.84
08cg142	36.5230	-114.4278	377.2	979658.62	-88.40	0.02	0.24	-130.87	-24.07
08cg143	36.5243	-114.4257	376.3	979658.84	-88.58	0.02	0.24	-130.94	-24.08
08cg144	36.5358	-114.4440	385.8	979657.13	-88.36	0.05	0.27	-131.76	-24.83
08cg145	36.5357	-114.4457	388.0	979657.05	-87.74	0.07	0.29	-131.38	-24.46
08cg146	36.5372	-114.4565	402.2	979654.99	-85.56	0.14	0.33	-130.76	-23.91
08cg147	36.5372	-114.4540	399.0	979655.44	-86.07	0.12	0.31	-130.93	-24.06

08cg148	36.5372	-114.4513	396.6	979655.68	-86.58	0.09	0.29	-131.19	-24.30
08cg149	36.5373	-114.4500	393.2	979656.39	-86.94	0.09	0.30	-131.16	-24.27
08cg150	36.7047	-114.6628	539.2	979657.11	-55.66	0.04	0.12	-116.56	-2.15
08cg151	36.7058	-114.6663	532.2	979659.15	-55.87	0.04	0.15	-115.95	-1.42
08cg152	36.7062	-114.6695	520.5	979662.59	-56.07	0.13	0.29	-114.69	-0.05
08cg153	36.7045	-114.6728	518.0	979664.26	-55.02	0.09	0.27	-113.38	1.25
08cg154	36.7038	-114.6770	515.1	979665.74	-54.41	0.06	0.28	-112.42	2.27
08cg155	36.7038	-114.6795	516.1	979666.15	-53.66	0.04	0.28	-111.79	2.97
08cg156	36.7060	-114.6815	517.6	979666.81	-52.74	0.04	0.29	-111.03	3.86
08cg157	36.7060	-114.6833	517.7	979667.32	-52.20	0.04	0.29	-110.49	4.43
08cg158	36.7087	-114.6837	518.3	979667.53	-52.02	0.05	0.31	-110.37	4.66
08cg159	36.7112	-114.6873	520.2	979668.17	-51.01	0.05	0.33	-109.56	5.67
08lr001	36.5005	-114.4703	423.4	979646.73	-84.09	0.30	0.53	-131.49	-25.60
08lr002	36.5022	-114.4670	440.4	979644.29	-81.43	0.11	0.23	-131.05	-25.12
08lr003	36.5053	-114.4625	432.9	979646.84	-81.48	0.17	0.29	-130.20	-24.17
08lr004	36.5068	-114.4600	428.5	979647.99	-81.82	0.20	0.32	-130.01	-23.94
08lr005	36.5105	-114.4570	409.3	979652.77	-83.29	0.10	0.28	-129.33	-23.14
08lr006	36.5127	-114.4553	403.4	979654.24	-83.80	0.11	0.31	-129.16	-22.88
08lr007	36.5137	-114.4538	401.4	979654.83	-83.93	0.11	0.31	-129.06	-22.75
08lr008	36.5152	-114.4510	396.5	979656.15	-84.26	0.09	0.29	-128.86	-22.48
08lr009	36.5163	-114.4480	393.0	979656.92	-84.65	0.09	0.29	-128.86	-22.43
08lr010	36.5168	-114.4452	391.0	979657.18	-85.05	0.08	0.28	-129.04	-22.57
08lr011	36.5173	-114.4417	388.4	979657.53	-85.56	0.05	0.24	-129.28	-22.79
08lr012	36.5183	-114.4397	386.7	979657.62	-86.06	0.05	0.25	-129.60	-23.06
08lr013	36.5195	-114.4372	384.5	979657.75	-86.72	0.08	0.28	-129.98	-23.39
08lr014	36.5200	-114.4348	382.7	979657.80	-87.27	0.05	0.25	-130.35	-23.71
08lr015	36.5207	-114.4328	381.7	979657.88	-87.56	0.03	0.23	-130.54	-23.85
08lr016	36.8067	-114.8513	751.5	979620.64	-35.47	3.88	4.39	-116.06	8.52
08lr017	36.8032	-114.8502	739.2	979624.32	-35.28	1.00	1.52	-117.36	7.04
08lr018	36.7998	-114.8527	728.0	979624.87	-37.88	0.75	1.29	-118.93	5.43
08lr019	36.7967	-114.8548	718.0	979624.82	-40.77	0.62	1.18	-120.79	3.54
08lr020	36.7937	-114.8548	710.8	979625.94	-41.59	0.60	1.18	-120.81	3.39
08lr021	36.7917	-114.8573	708.9	979625.02	-42.94	0.20	0.79	-122.33	1.89
08lr022	36.7623	-114.8630	640.7	979641.55	-44.90	0.55	1.77	-115.61	7.73
08lr023	36.7637	-114.8623	636.0	979642.22	-45.79	0.41	1.64	-116.10	7.27
08lr024	36.7652	-114.8615	636.0	979641.74	-46.40	0.26	1.47	-116.88	6.51
08lr025	36.7665	-114.8610	637.8	979641.06	-46.64	0.17	1.34	-117.45	5.96
08lr026	36.7675	-114.8605	640.6	979640.29	-46.64	0.13	1.27	-117.84	5.58
08lr027	36.7698	-114.8592	646.5	979638.54	-46.76	0.07	1.11	-118.79	4.66
08lr028	36.7710	-114.8570	650.8	979637.28	-46.80	0.07	1.04	-119.39	4.03
08lr029	36.7730	-114.8545	660.3	979635.20	-46.11	0.05	0.90	-119.91	3.47
08lr030	36.7762	-114.8538	666.5	979633.66	-46.04	0.06	0.84	-120.59	2.90
08lr031	36.7787	-114.8538	672.9	979632.22	-45.72	0.06	0.79	-121.04	2.51
08lr032	36.7808	-114.8542	678.1	979630.99	-45.54	0.08	0.78	-121.46	2.20
08lr033	36.7833	-114.8547	685.8	979629.25	-45.10	0.10	0.76	-121.91	1.86
08lr034	36.7862	-114.8545	693.2	979628.18	-44.15	0.15	0.78	-121.77	2.10
08lr035	36.7885	-114.8550	700.4	979627.13	-43.17	0.17	0.78	-121.61	2.37
08lr036	36.7910	-114.8542	709.3	979626.10	-41.66	0.22	0.80	-121.09	2.95
08lr037	36.6488	-114.6487	532.3	979655.71	-54.35	0.16	0.18	-114.41	-2.65
08lr038	36.6555	-114.6413	485.8	979666.46	-58.53	0.06	0.18	-113.32	-1.46
08lr039	36.6592	-114.6360	483.1	979667.88	-58.24	0.07	0.20	-112.72	-0.81
08lr040	36.6612	-114.6267	492.3	979666.82	-56.66	0.03	0.10	-112.27	-0.45

08lr041	36.6663	-114.6242	495.1	979666.23	-56.84	0.07	0.13	-112.74	-0.76
08lr042	36.6695	-114.6227	499.7	979665.31	-56.61	0.05	0.09	-113.07	-0.98
08lr043	36.6733	-114.6203	516.5	979661.82	-55.23	0.04	0.04	-113.64	-1.44
08lr044	36.6997	-114.6225	513.8	979660.07	-60.09	0.06	0.12	-118.12	-4.65
08lr045	36.6963	-114.6227	525.2	979657.57	-58.79	0.04	0.07	-118.16	-4.85
08lr046	36.6943	-114.6228	526.1	979657.65	-58.25	0.03	0.05	-117.74	-4.51
08lr047	36.6912	-114.6218	524.3	979658.43	-57.77	0.02	0.04	-117.06	-3.99
08lr048	36.6888	-114.6197	522.7	979658.87	-57.62	0.02	0.03	-116.73	-3.78
08lr049	36.6863	-114.6197	521.1	979659.58	-57.17	0.02	0.03	-116.11	-3.28
08lr050	36.6835	-114.6198	519.9	979660.16	-56.72	0.02	0.03	-115.53	-2.84
08lr051	36.6805	-114.6193	517.7	979660.85	-56.46	0.02	0.03	-115.02	-2.48
08lr052	36.6778	-114.6198	511.0	979662.77	-56.37	0.03	0.05	-114.16	-1.74
08lr054	36.4460	-114.3588	371.3	979652.96	-89.22	0.14	0.41	-130.86	-24.23
08lr055	36.4448	-114.3628	386.1	979650.66	-86.88	0.26	0.47	-130.12	-23.62
08lr056	36.4435	-114.3653	394.0	979649.43	-85.55	0.21	0.39	-129.76	-23.35
08lr057	36.4425	-114.3692	405.2	979647.95	-83.47	0.22	0.37	-128.98	-22.66
08lr058	36.4423	-114.3735	422.1	979645.72	-80.47	0.42	0.53	-127.72	-21.52
08lr059	36.4415	-114.3760	430.0	979645.04	-78.66	0.28	0.38	-126.95	-20.83
08lr060	36.4400	-114.3800	444.9	979643.52	-75.43	0.23	0.32	-125.47	-19.49
08lr061	36.4395	-114.3840	454.9	979643.87	-71.95	0.30	0.39	-123.06	-17.17
08lr062	36.4400	-114.3897	436.8	979652.31	-69.16	0.16	0.23	-118.37	-12.64
08lr063	36.4400	-114.3933	420.6	979657.89	-68.57	0.15	0.24	-115.94	-10.30
08lr064	36.4400	-114.3958	422.0	979658.53	-67.50	0.12	0.21	-115.06	-9.48
08lr065	36.4383	-114.4027	418.4	979660.54	-66.45	0.09	0.19	-113.62	-8.20
08lr066	36.4375	-114.4073	418.2	979661.06	-65.93	0.07	0.19	-113.09	-7.76
08lr067	36.4705	-114.3845	379.3	979664.87	-76.98	0.11	0.28	-119.64	-13.22
08lr068	36.4677	-114.3860	382.6	979664.19	-76.37	0.05	0.21	-119.49	-13.16
08lr069	36.4677	-114.3887	390.0	979662.83	-75.48	0.06	0.19	-119.43	-13.14
08lr070	36.4673	-114.3913	394.2	979662.07	-74.89	0.05	0.17	-119.35	-13.13
08lr071	36.4673	-114.3937	400.8	979660.78	-74.16	0.07	0.17	-119.36	-13.18
08lr072	36.4660	-114.3968	407.3	979659.53	-73.28	0.07	0.16	-119.23	-13.13
08lr073	36.4660	-114.3993	413.2	979658.25	-72.74	0.07	0.15	-119.37	-13.33
08lr074	36.4647	-114.4022	408.3	979659.32	-73.07	0.15	0.24	-119.05	-13.08
08lr075	36.4632	-114.4042	417.9	979657.50	-71.81	0.07	0.14	-118.97	-13.06
08lr076	36.4618	-114.4080	418.7	979657.50	-71.43	0.06	0.14	-118.69	-12.90
08lr077	36.4605	-114.4108	425.2	979656.21	-70.62	0.07	0.14	-118.60	-12.92
08lr078	36.4588	-114.4130	428.7	979655.90	-69.69	0.06	0.13	-118.09	-12.46
08lr079	36.4565	-114.4148	431.0	979656.20	-68.47	0.07	0.14	-117.13	-11.56
08lr080	36.4540	-114.4168	435.6	979656.21	-66.85	0.07	0.14	-116.01	-10.51
08lr081	36.4505	-114.4182	439.8	979656.71	-64.75	0.06	0.13	-114.40	-9.00
08lr082	36.4490	-114.4193	444.5	979656.32	-63.56	0.05	0.11	-113.76	-8.40
08lr083	36.4465	-114.4218	451.9	979655.31	-62.05	0.06	0.12	-113.09	-7.81
08lr084	36.4435	-114.4235	458.0	979654.54	-60.68	0.06	0.11	-112.41	-7.21
08lr085	36.4408	-114.4267	467.5	979652.68	-59.38	0.05	0.10	-112.20	-7.09
08lr086	36.5523	-114.3707	545.3	979625.73	-71.96	0.21	0.28	-133.39	-24.65
08lr087	36.5448	-114.3663	549.2	979626.18	-69.67	0.15	0.26	-131.56	-22.92
08lr088	36.5347	-114.3843	566.1	979619.67	-70.08	0.69	0.87	-133.27	-25.33
08lr089	36.5427	-114.3908	569.4	979617.16	-72.27	1.11	1.25	-135.45	-27.47
08lr090	36.5907	-114.3910	560.5	979618.07	-78.25	0.02	0.00	-141.68	-32.33
08lr091	36.5875	-114.3988	565.2	979616.38	-78.21	0.07	0.07	-142.11	-33.05
08lr092	36.4887	-114.3242	357.7	979657.35	-92.72	0.90	1.47	-131.75	-23.16
08lr093	36.4895	-114.3178	370.4	979654.41	-91.81	0.69	1.25	-132.50	-23.67

08lr094	36.4947	-114.3133	389.7	979652.02	-88.70	0.61	1.15	-131.67	-22.59
08lr095	36.4973	-114.3070	409.3	979648.50	-86.40	0.22	0.74	-131.99	-22.62
08lr096	36.5020	-114.3027	423.7	979646.92	-83.95	0.30	0.83	-131.08	-21.47
08lr097	36.5102	-114.2960	450.8	979646.17	-77.03	0.31	0.86	-127.20	-17.11
08lr098	36.6963	-114.6815	511.9	979666.43	-54.03	0.06	0.31	-111.65	2.82
08lr099	36.7125	-114.7150	539.5	979669.49	-43.87	0.19	0.64	-104.28	11.76
08lr100	36.7112	-114.7127	538.3	979669.35	-44.25	0.19	0.62	-104.55	11.34
08lr101	36.7108	-114.7100	532.5	979670.11	-45.27	0.21	0.64	-104.89	10.91
08lr102	36.7105	-114.7078	538.0	979668.57	-45.08	0.15	0.52	-105.43	10.30
08lr103	36.7110	-114.7010	526.6	979669.46	-47.75	0.27	0.63	-106.71	8.89
08lr104	36.7110	-114.6990	526.6	979668.94	-48.27	0.14	0.48	-107.38	8.17
08lr105	36.7110	-114.6970	525.1	979668.70	-48.97	0.09	0.42	-107.97	7.52
08lr106	36.7110	-114.6950	521.8	979668.93	-49.76	0.08	0.41	-108.40	7.03
08lr107	36.7112	-114.6927	521.8	979668.42	-50.26	0.06	0.37	-108.95	6.42
08lr108	36.7112	-114.6907	520.7	979668.38	-50.65	0.06	0.36	-109.22	6.10

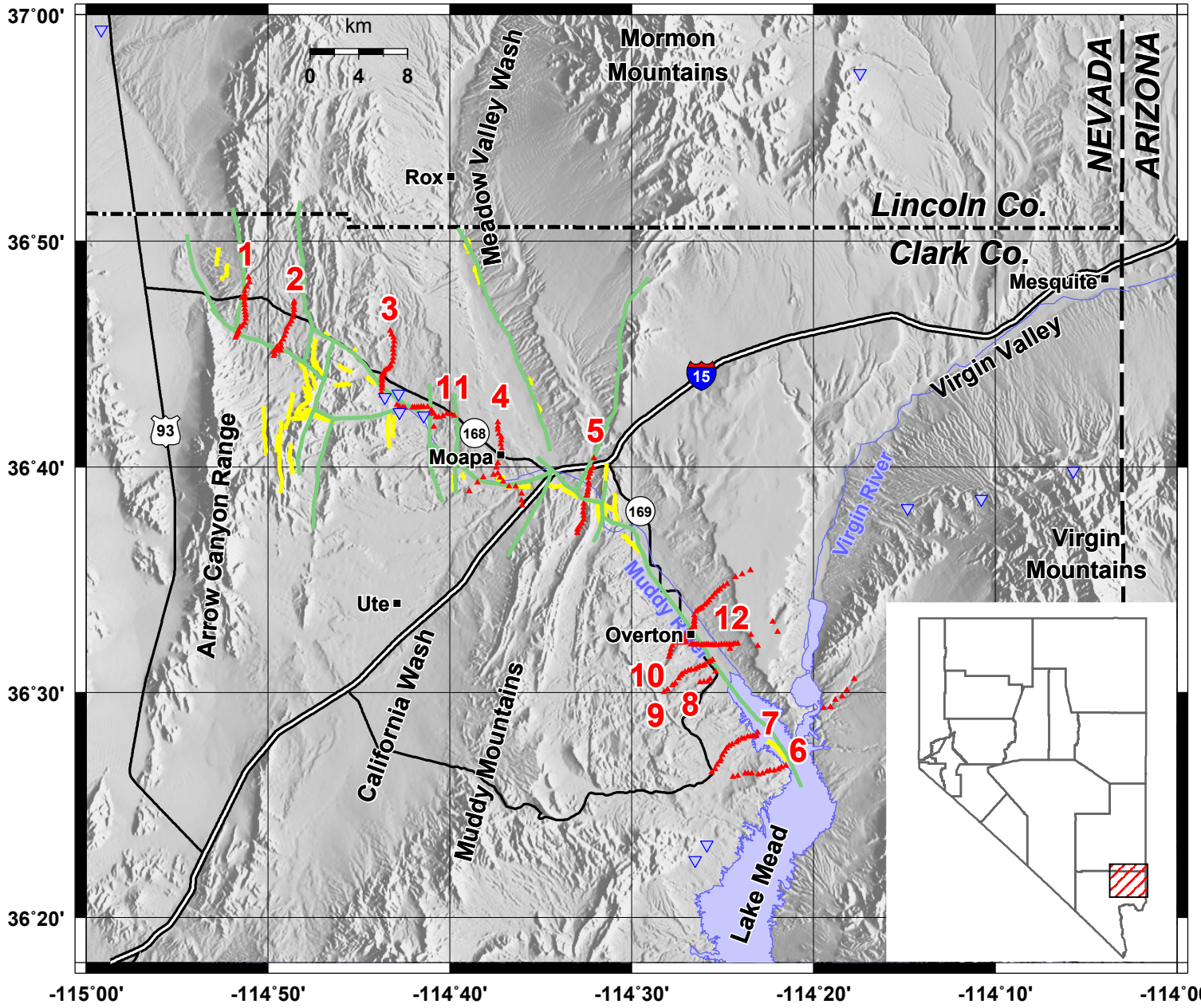

Figure 1. Shaded-relief map of the study area in the Moapa Valley region of southern Nevada. Red triangles indicate gravity station locations collected in March 2008, with traverses numbered. Green lines indicate the "terminus" newly-mapped faults, and yellow lines indicate the "GE7C" newly-mapped faults. Blue triangles denote spring locations. Inset shows study area (hachured box) within Nevada.

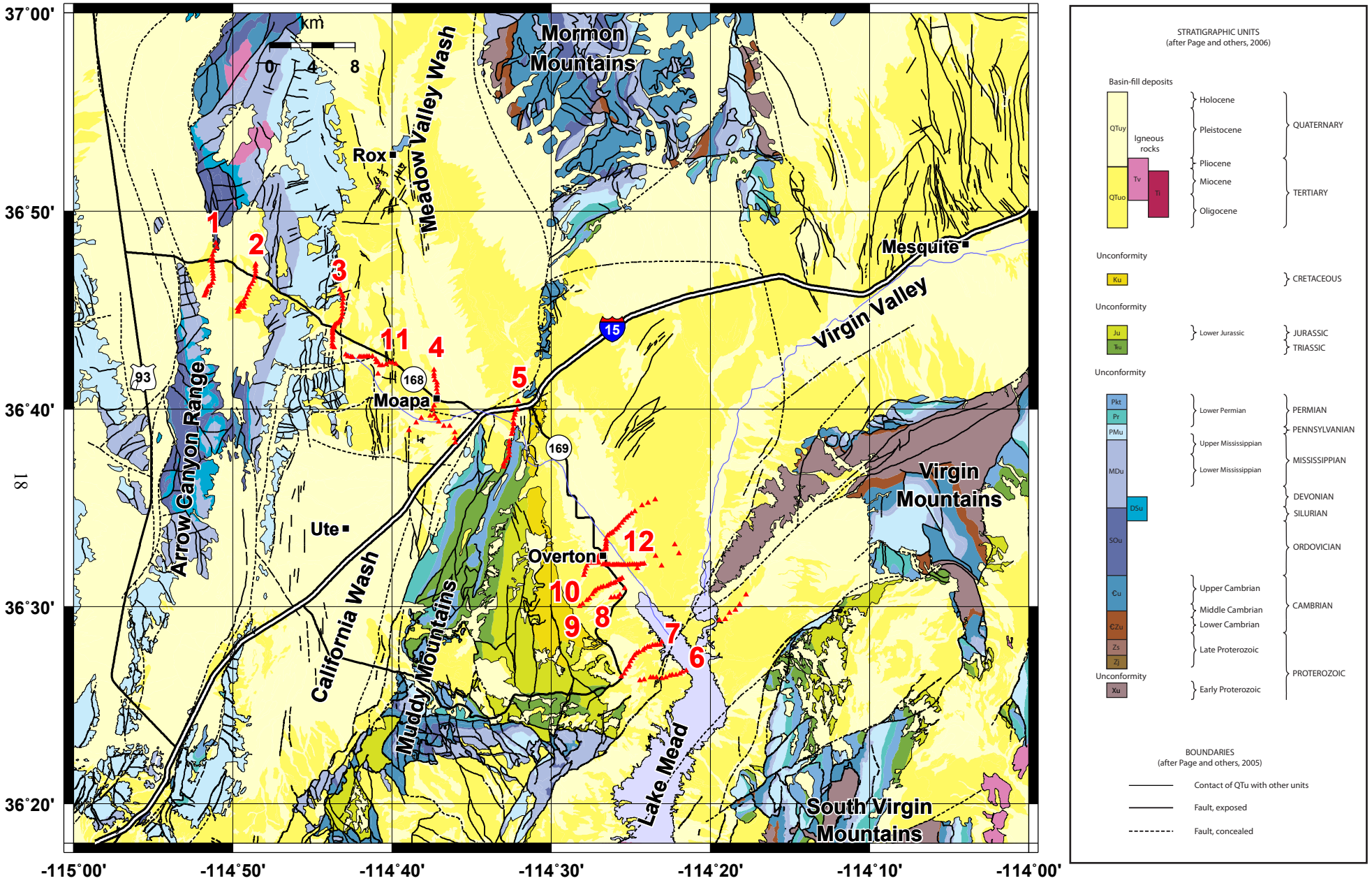

Figure 2. Geologic map of the study area modified from Page and others (2005); the grouping of geologic units is based on Page and others (2006). We subdivide the Page and others (2006) QTu sedimentary unit into younger (QTuy, middle Pleistocene and younger) and older (QTuo, early Pleistocene and older) units. March 2008 gravity stations are indicated in red.

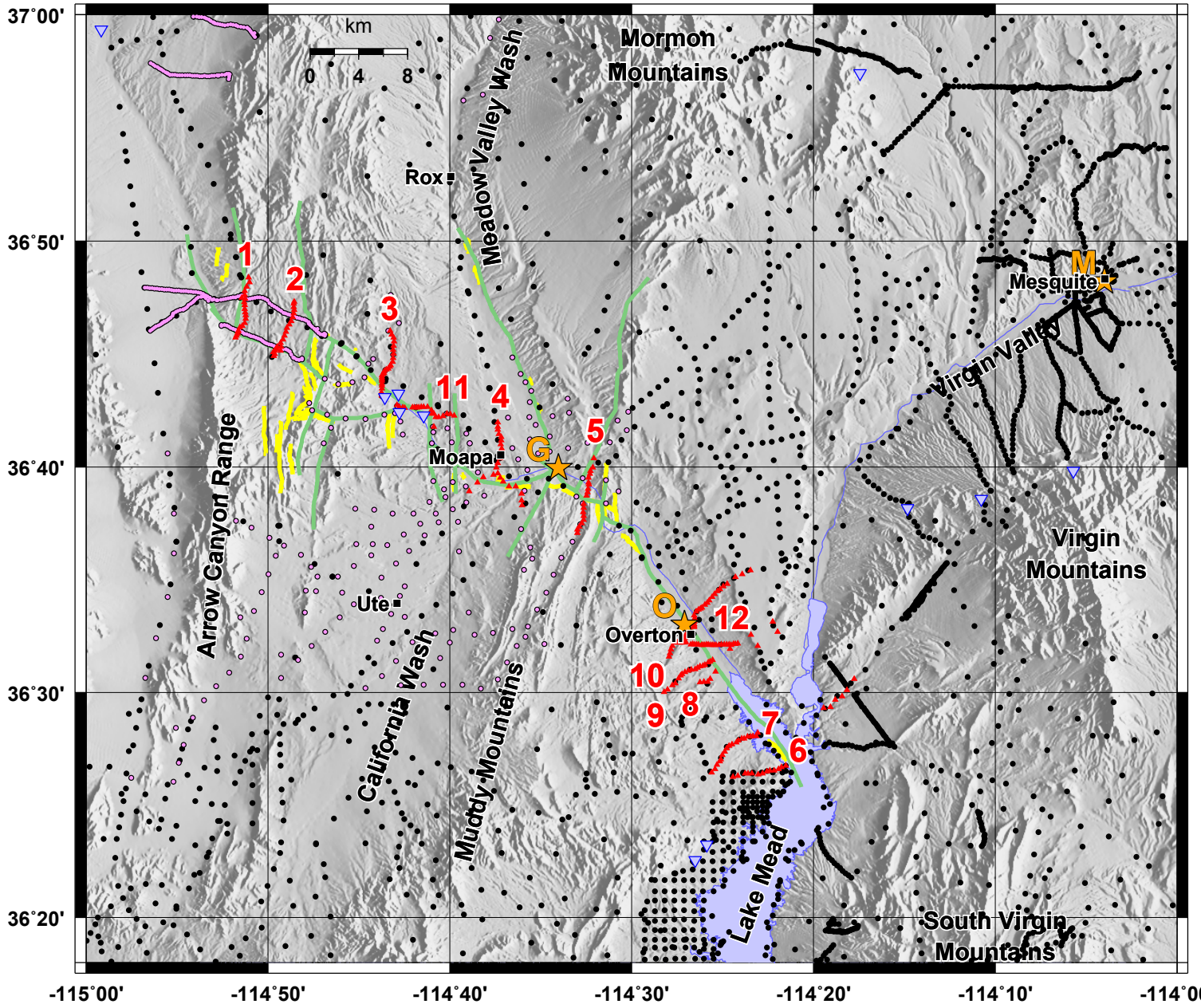

Figure 3. Gravity station locations in the study area. Red triangles indicate March 2008 gravity stations. Stations collected by the USGS using gravity base station GLEN are denoted in pink and other stations are denoted in black. Orange stars indicate the locations of gravity base stations (O=OVER; G=GLEN; M=MESCN). Green lines indicate the "terminus" newly-mapped faults, and yellow lines indicate the "GE7C" newly-mapped faults. Blue triangles denote spring locations.

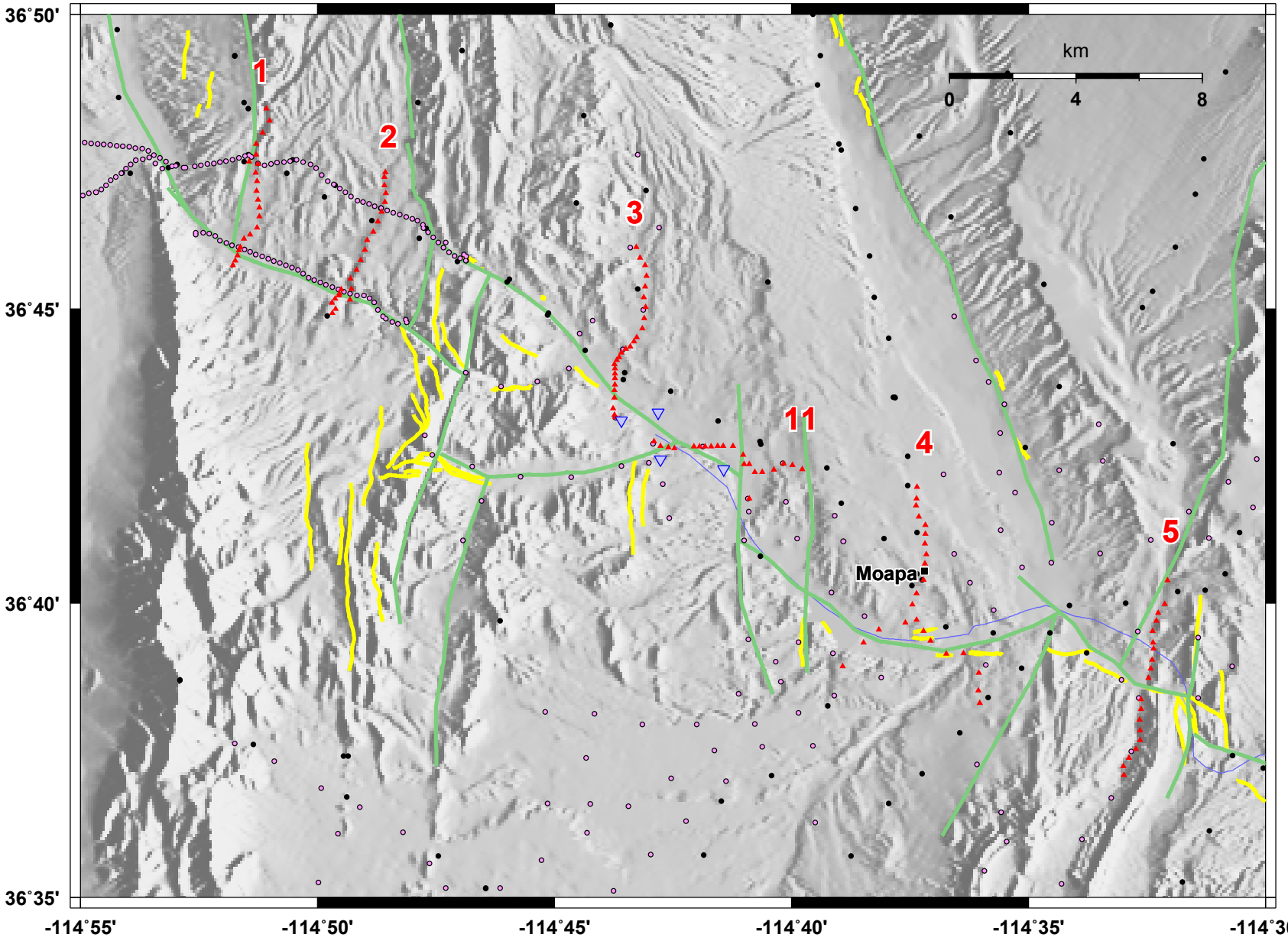

Figure 4. Shaded-relief map of the northwestern portion of the study area. Red triangles indicate gravity station locations collected in March 2008, with traverses labeled. Gravity stations collected by the USGS by using gravity base station GLEN are denoted in pink and other stations are denoted in black. Green lines indicate the "terminus" newly-mapped faults, and yellow lines indicate the "GE7C" newly-mapped faults. Blue triangles denote spring locations.

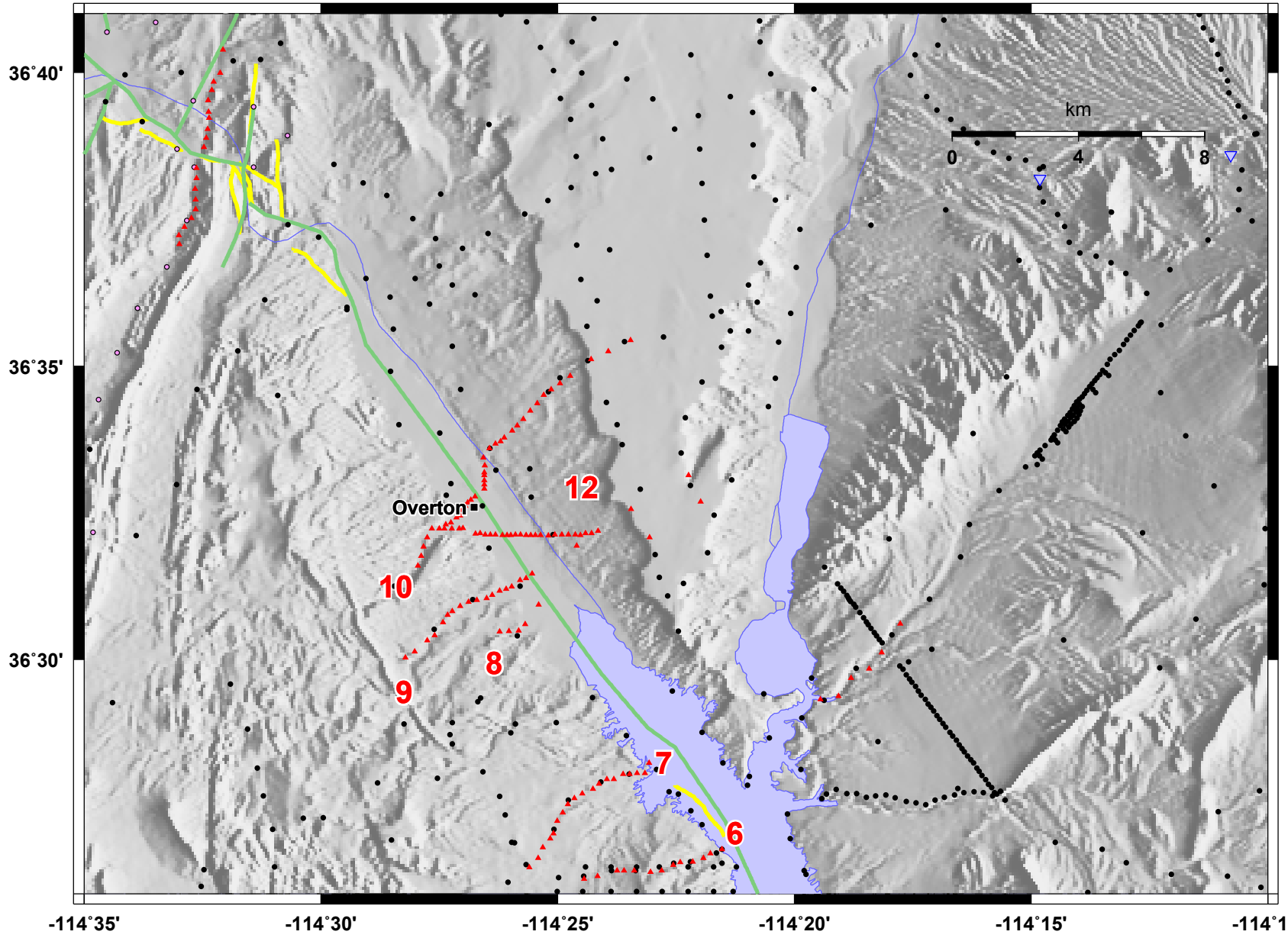

Figure 5. Shaded-relief map of the southeastern portion of the study area. Red triangles indicate gravity station locations collected in March 2008, with traverses labeled. Gravity stations collected by the USGS by using gravity base station GLEN are denoted in pink and other stations are denoted in black. Green lines indicate the "terminus" newly-mapped faults, and yellow lines indicate the "GE7C" newly-mapped faults. Blue triangles denote spring locations.

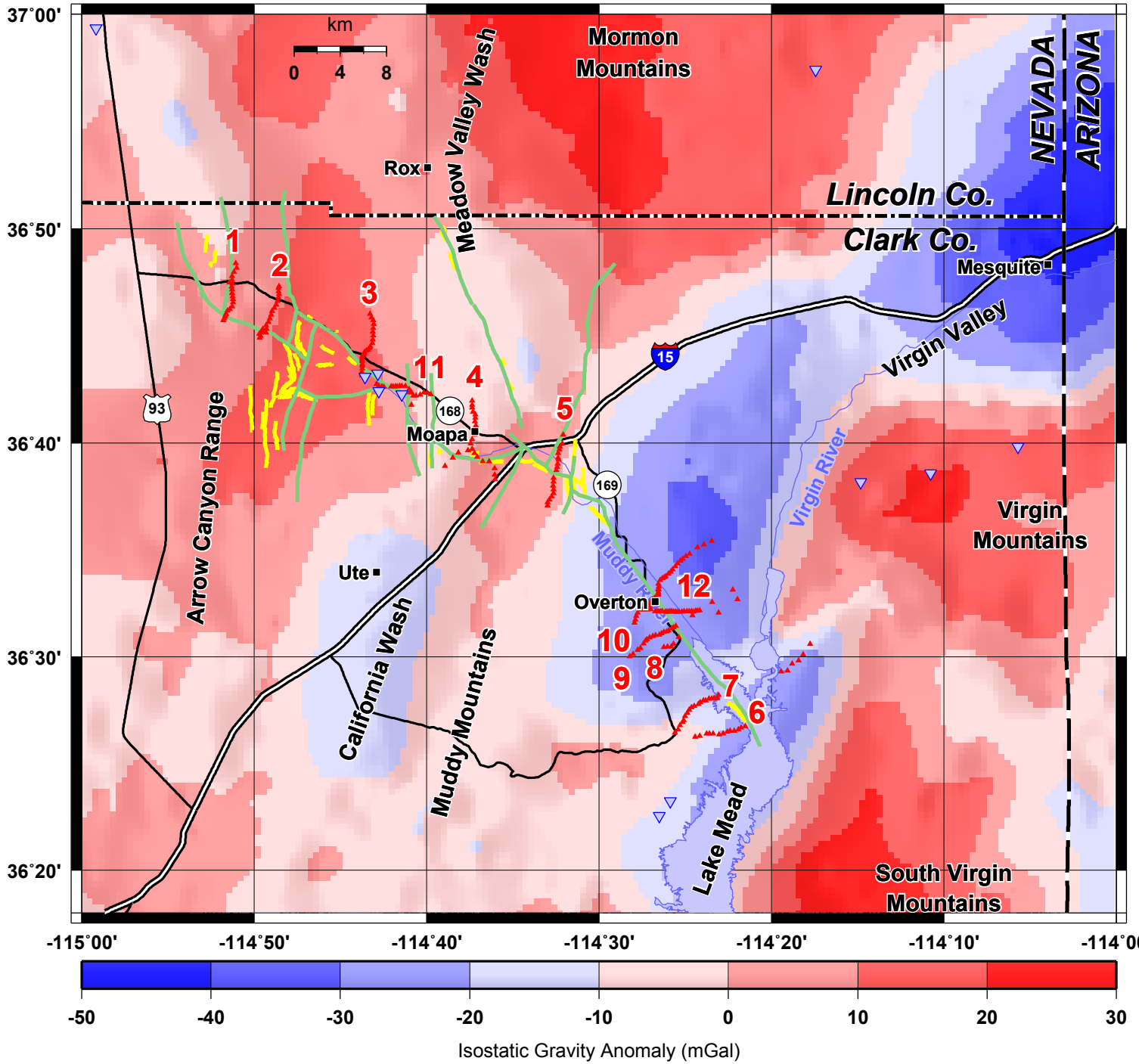

Figure 6. Isostatic gravity map of the study area, created with pre-March 2008 data. Red triangles indicate gravity station locations collected in March 2008, with traverses labeled. Green lines indicate the "terminus" newly-mapped faults, and yellow lines indicate the "GE7C" newly-mapped faults. Blue triangles denote spring locations.

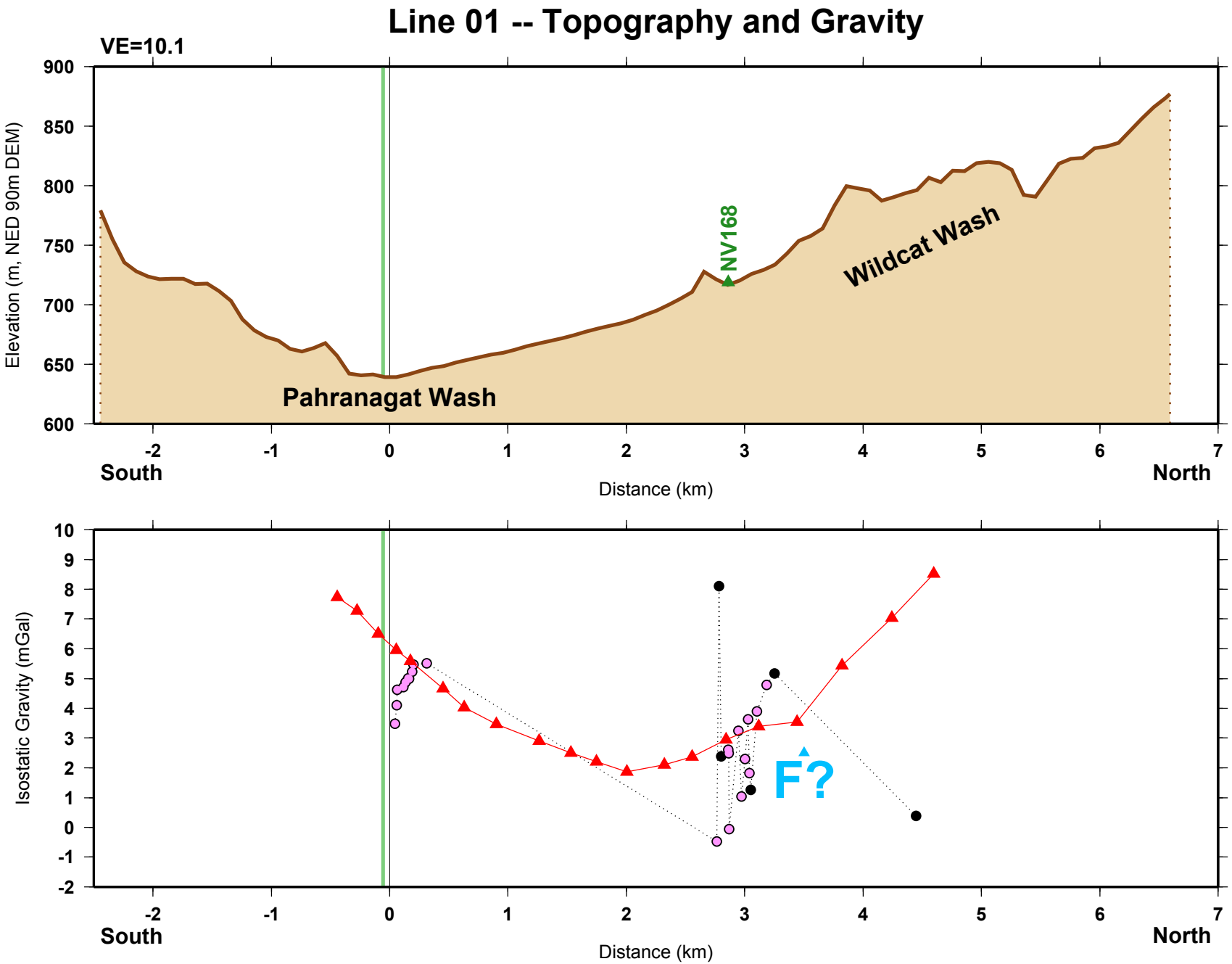

Figure 7. Gravity line 01. Top panel: Topography profile, with labels for physiographic features and road crossings (dark green; NV=Nevada route; I=Interstate route). Green lines indicate the traces of "terminus" newly-mapped faults, and yellow lines indicate the traces of "GE7C" newly-mapped faults. Bottom panel: I sostatic gravity profile. Red triangles indicate gravity station locations collected in March 2008, with traverses numbered. Gravity stations collected by the USGS using gravity base station GLEN are denoted in pink, and other stations are denoted in black. Green lines indicate the traces of "terminus" newly-mapped faults, and yellow lines indicate the traces of "GE7C" newly-mapped faults. Blue "F" labels indicate where buried faults are inferred from the gravity anomalies; "F?" labels indicate where buried faults are inferred to exist with less certainty.

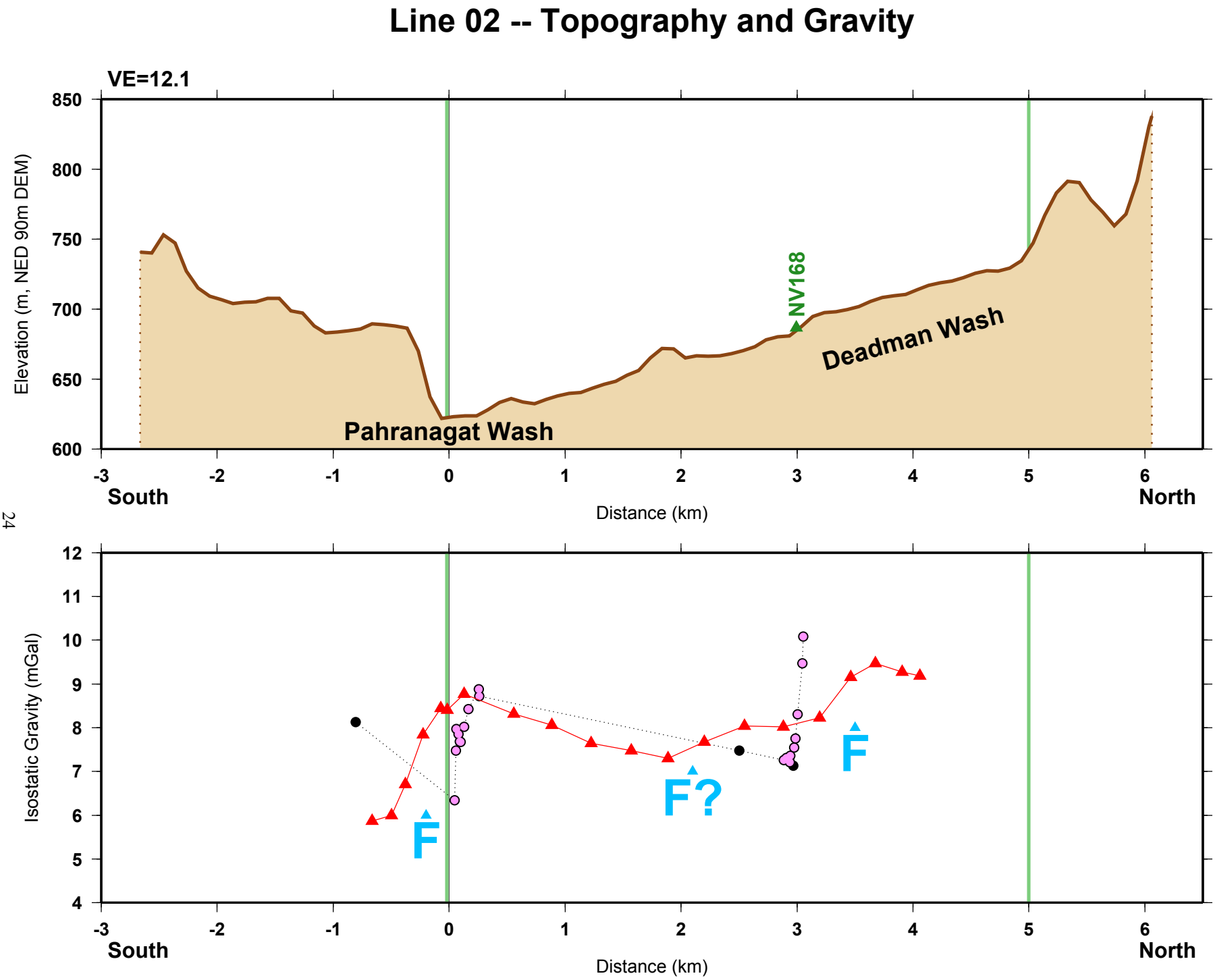

Figure 8. Gravity line 02. Top panel: Topography profile. Bottom panel: Isostatic gravity profile. Same labels as fig. 7.

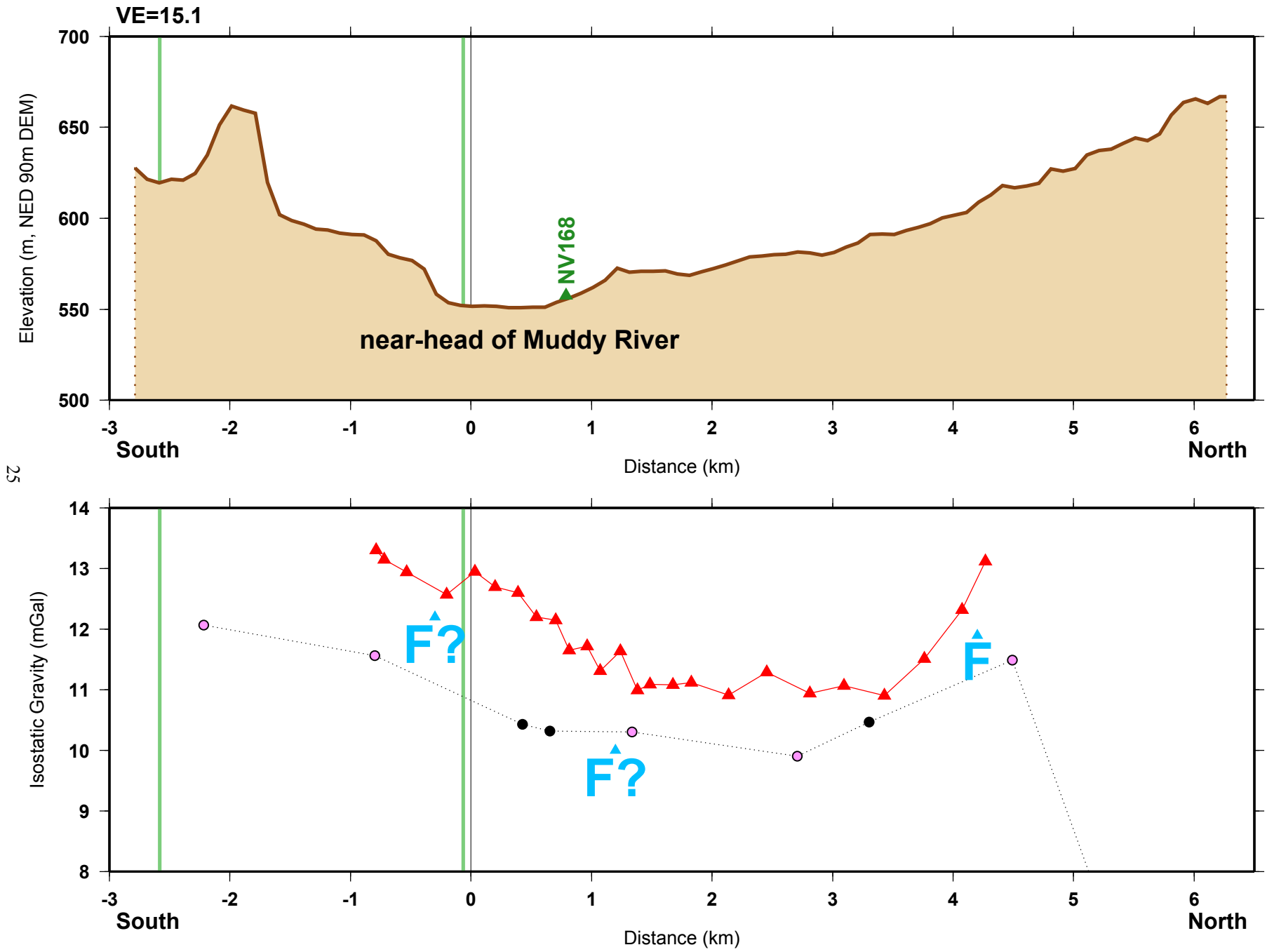

Figure 9. Gravity line 03. Top panel: Topography profile. Bottom panel: Isostatic gravity profile. Same labels as fig. 7.

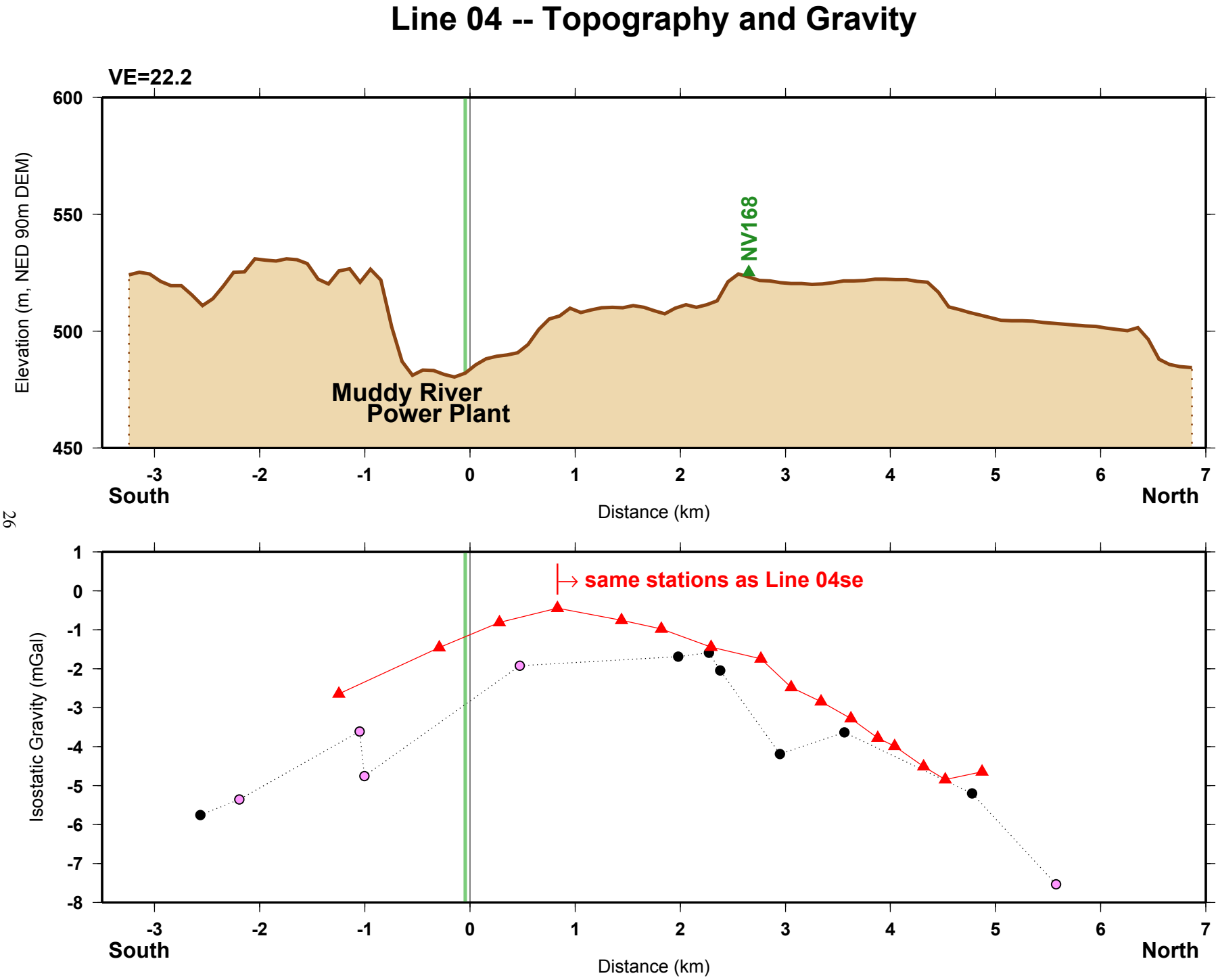

Figure 10. Gravity line 04. Top panel: Topography profile. Bottom panel: Isostatic gravity profile. Same labels as fig. 7.

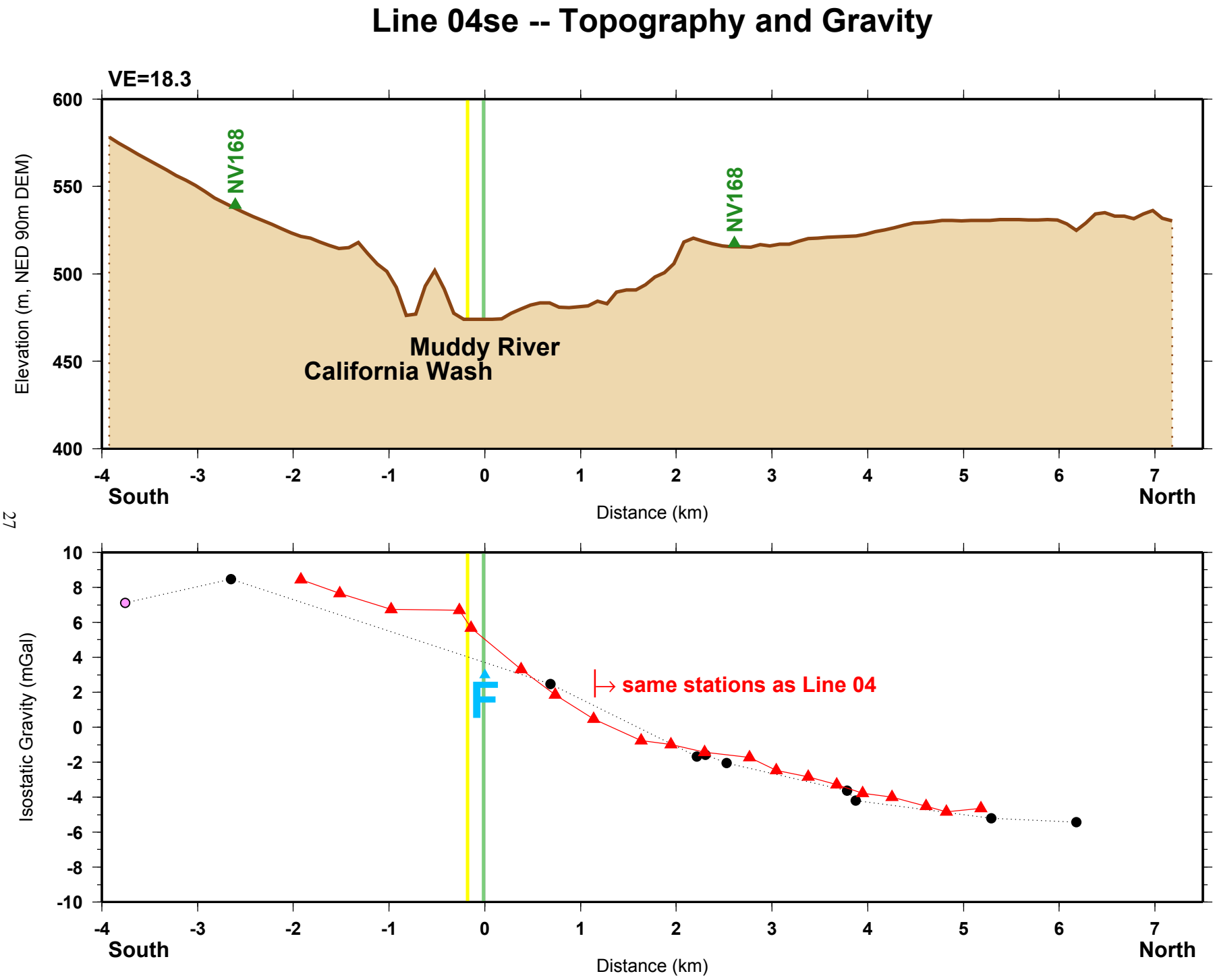

Figure 11. Gravity line 04se. Top panel: Topography profile. Bottom panel: Isostatic gravity profile. Same labels as fig. 7.

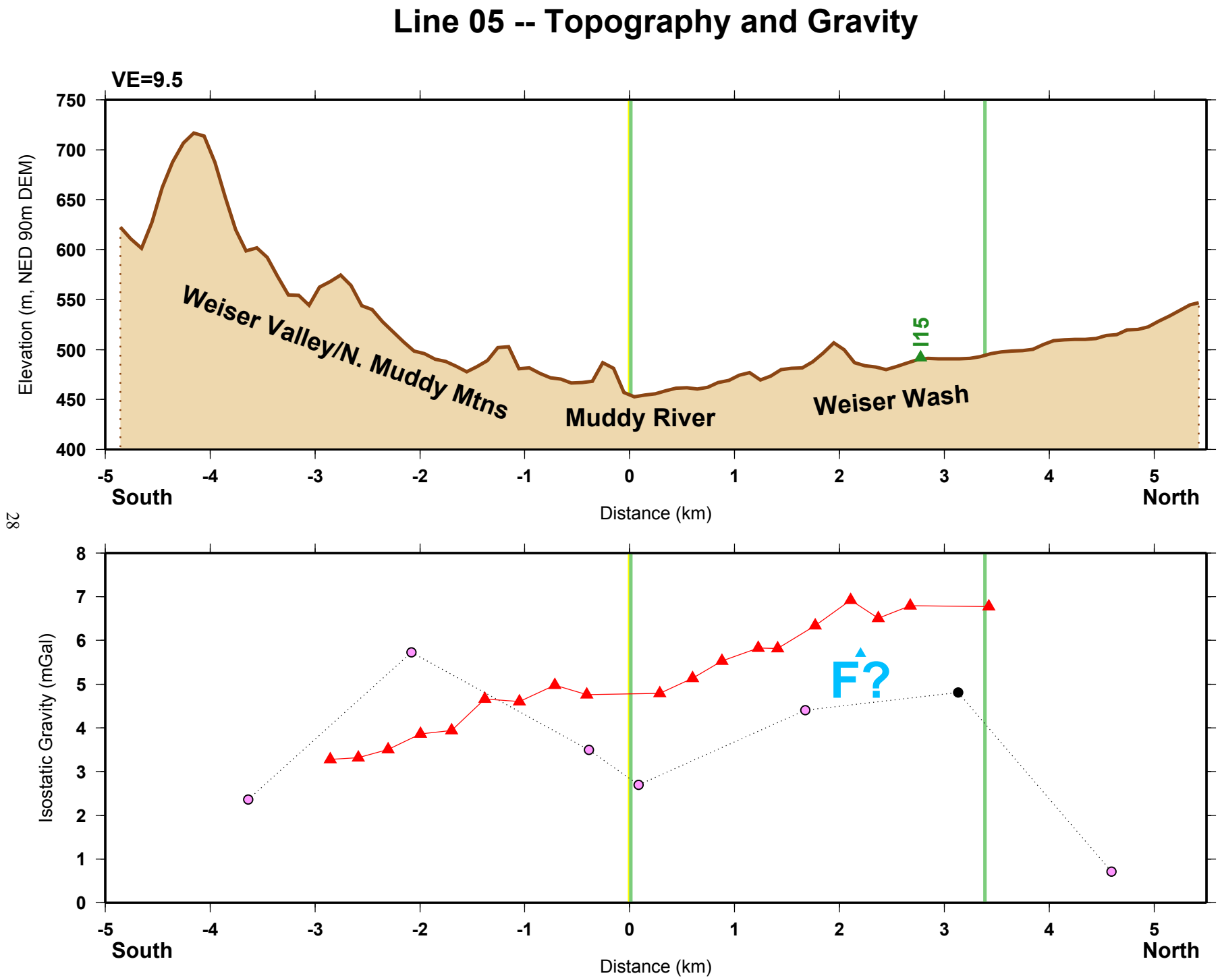

Figure 12. Gravity line 05. Top panel: Topography profile. Bottom panel: Isostatic gravity profile. Same labels as fig. 7.

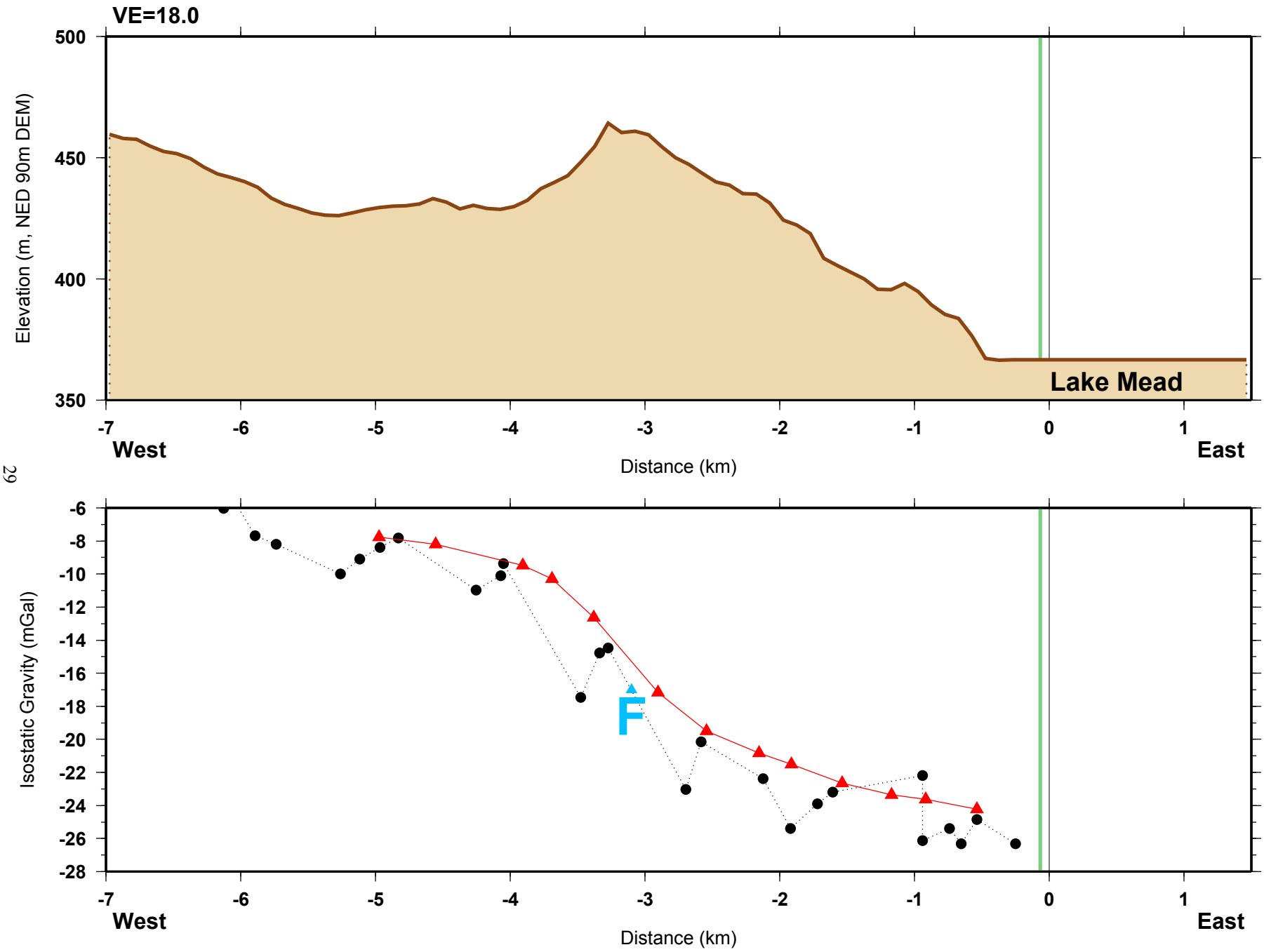

Figure 13. Gravity line 06. Top panel: Topography profile. Bottom panel: Isostatic gravity profile. Same labels as fig. 7.

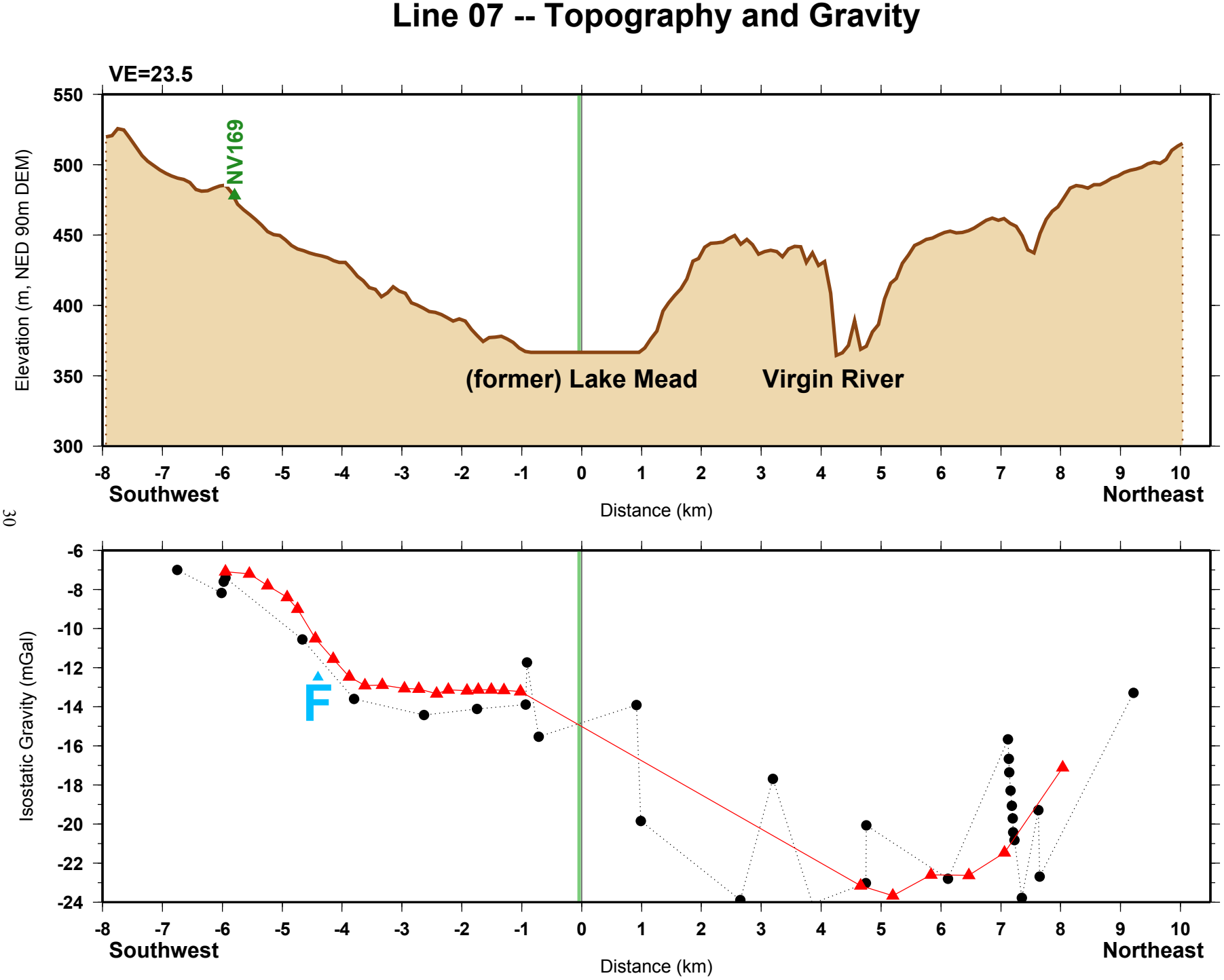

Figure 14. Gravity line 07. Top panel: Topography profile. Bottom panel: Isostatic gravity profile. Same labels as fig. 7.

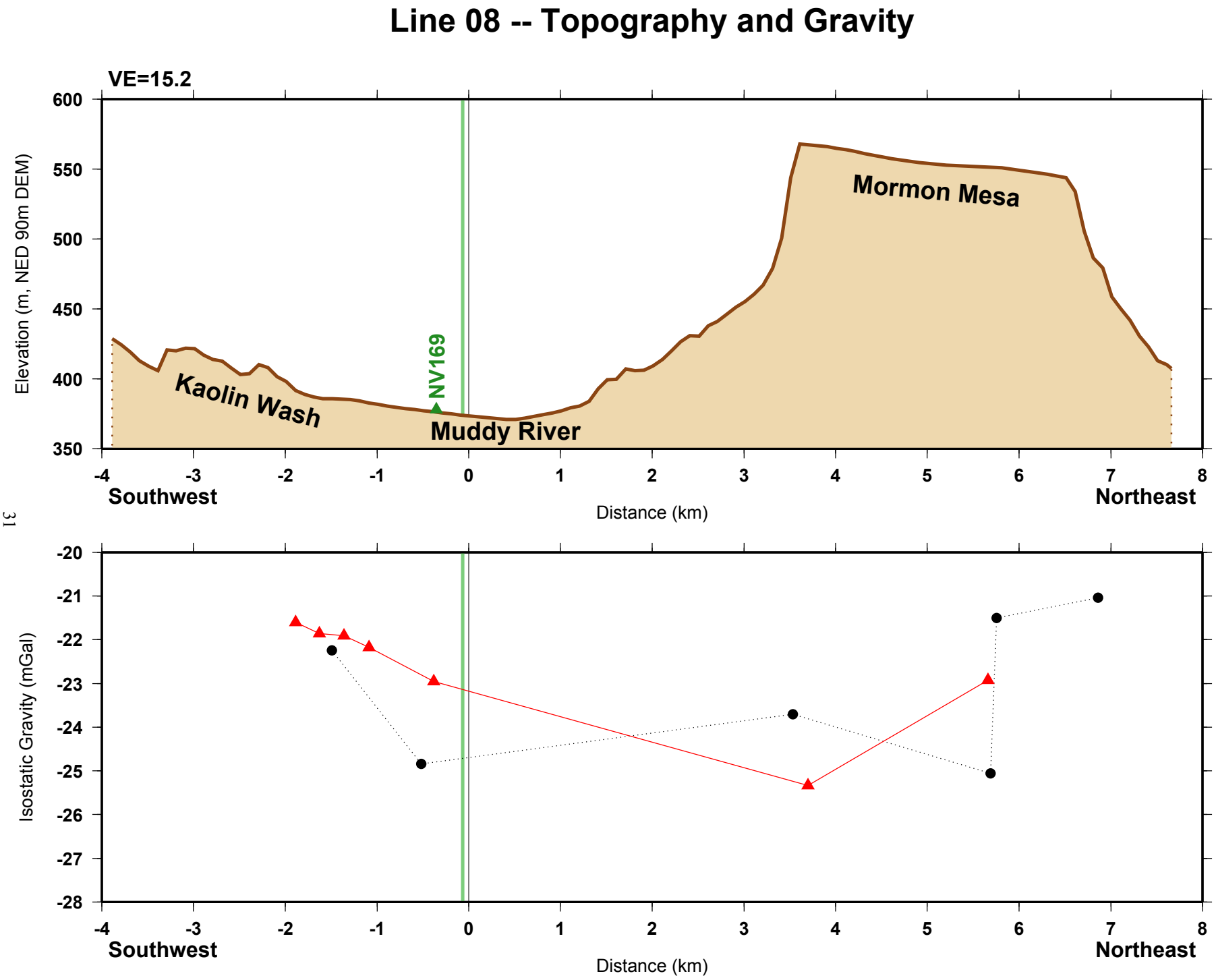

Figure 15. Gravity line 08. Top panel: Topography profile. Bottom panel: Isostatic gravity profile. Same labels as fig. 7.

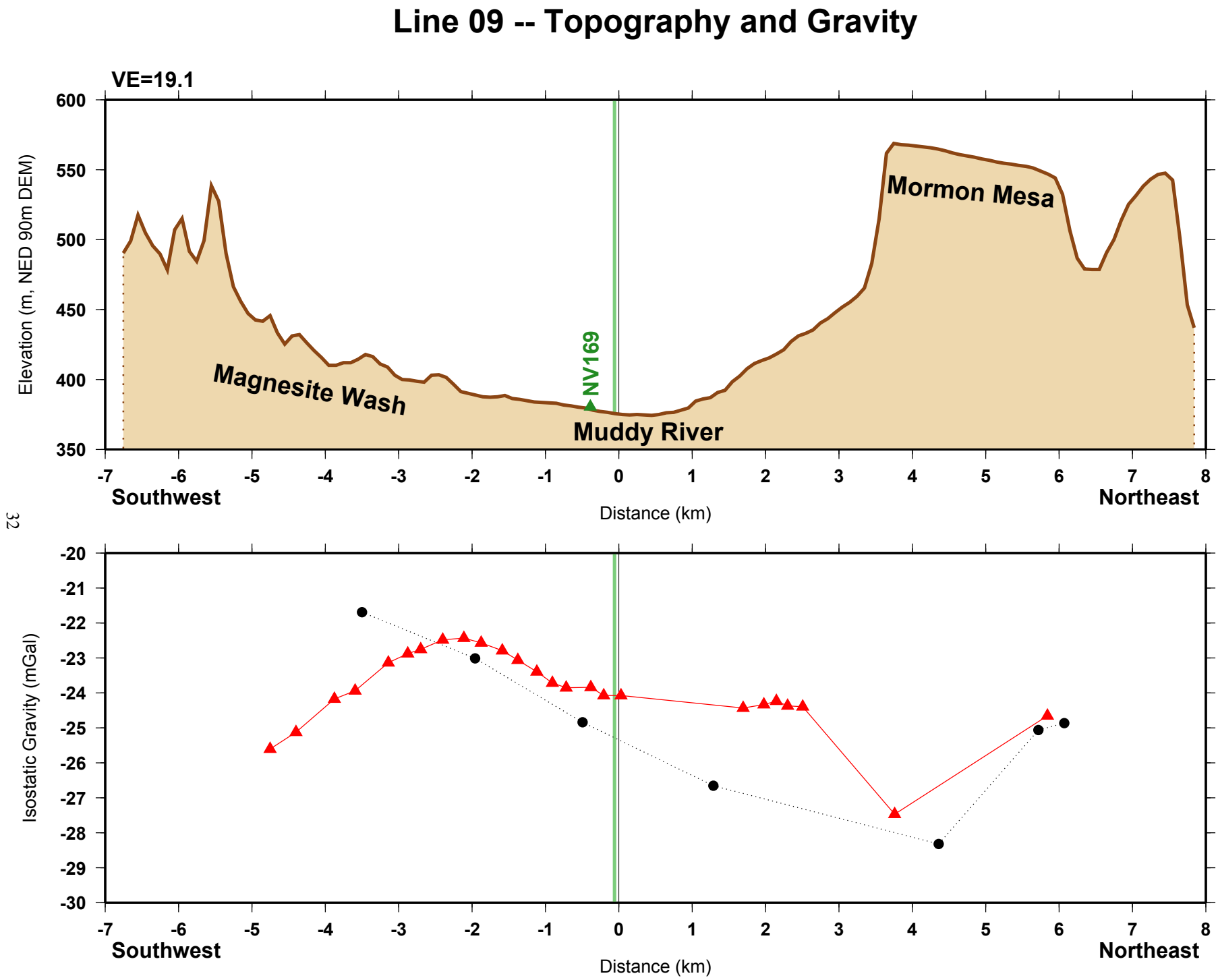

Figure 16. Gravity line 09. Top panel: Topography profile. Bottom panel: Isostatic gravity profile. Same labels as fig. 7.

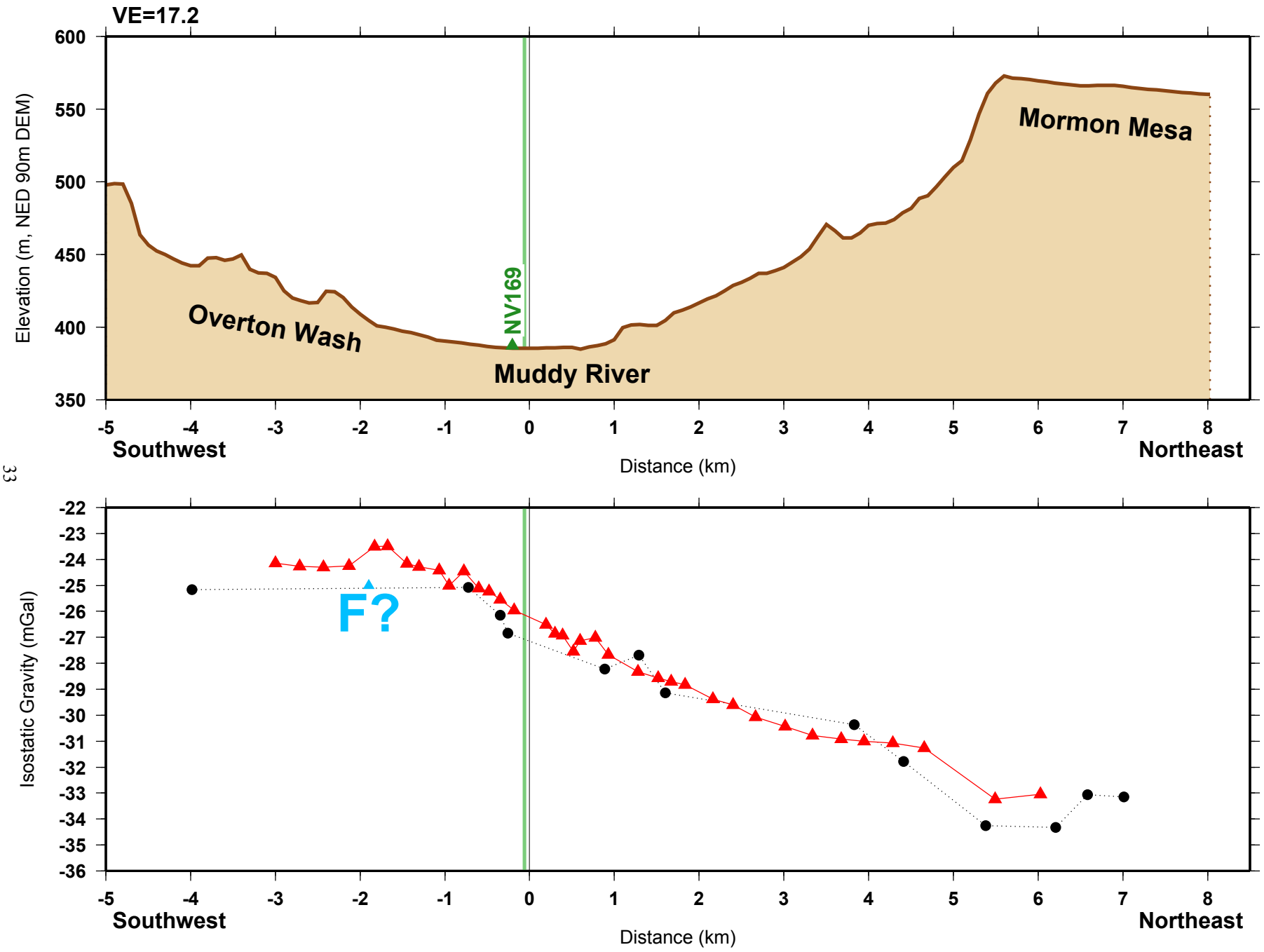

Figure 17. Gravity line 10. Top panel: Topography profile. Bottom panel: Isostatic gravity profile. Same labels as fig. 7.

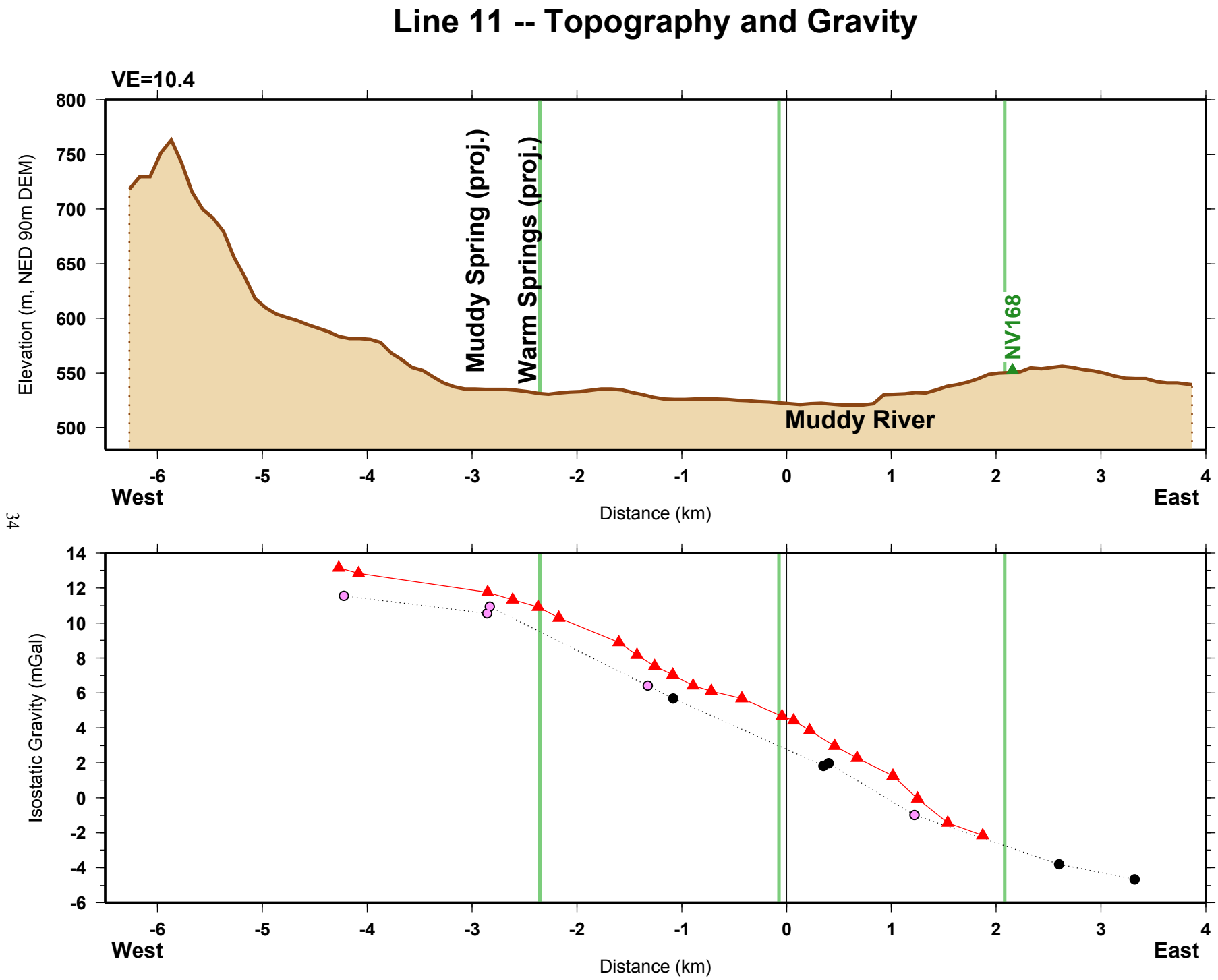

Figure 18. Gravity line 11. Top panel: Topography profile. Bottom panel: Isostatic gravity profile. Same labels as fig. 7. Label "(proj.)" indicates the projected locations of the springs onto the gravity line.

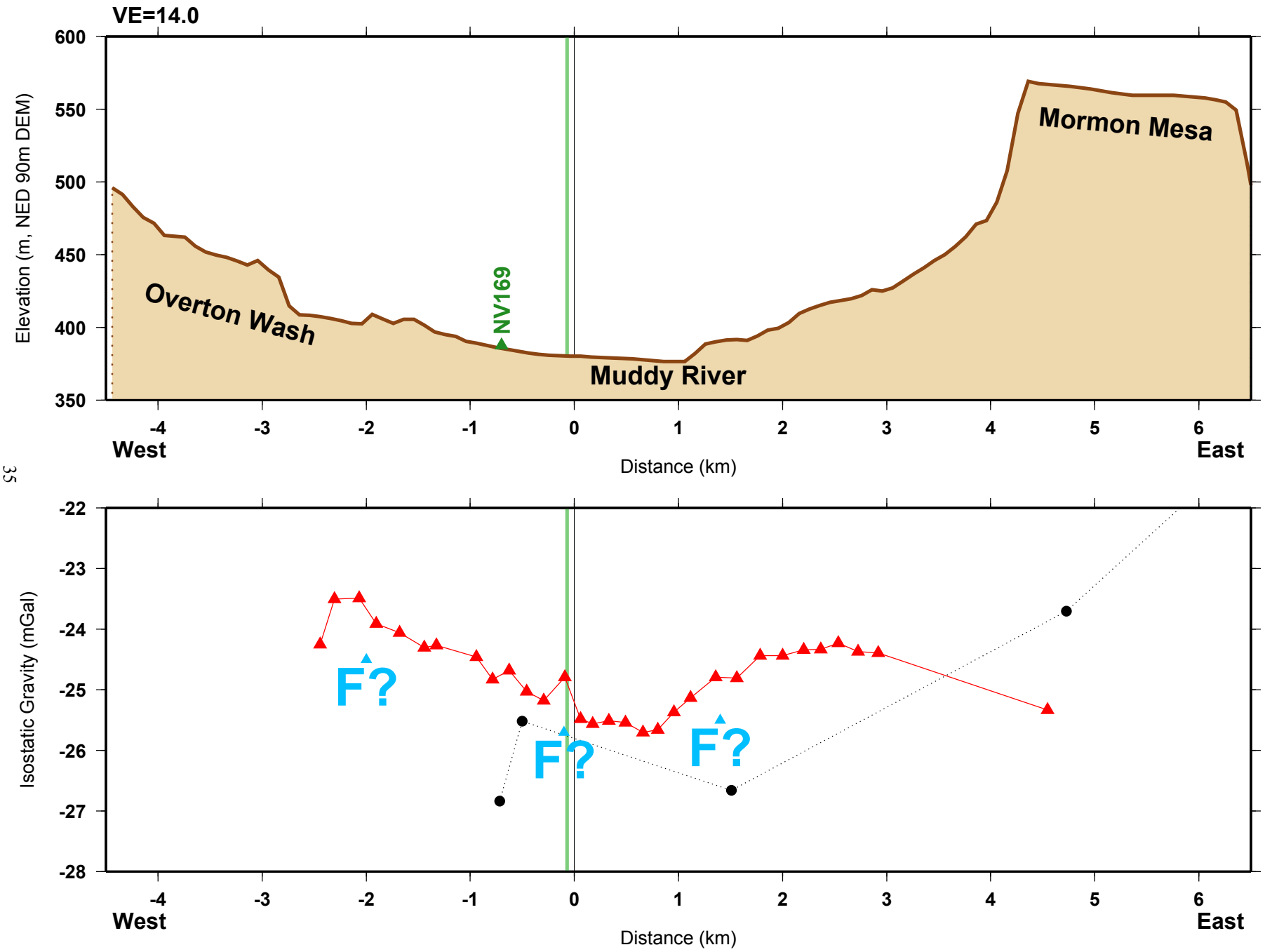

Figure 19. Gravity line 12. Top panel: Topography profile. Bottom panel: Isostatic gravity profile. Same labels as fig. 7.